

See discussions, stats, and author profiles for this publication at: <https://www.researchgate.net/publication/338924428>

Supersymmetric Dark Matter Searches with CMS Data

Thesis · October 2014

DOI: 10.13140/RG.2.2.13923.50724

CITATIONS
0

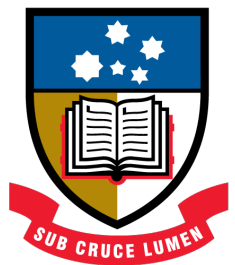
READS
1,457

1 author:



Daniel Murnane
Lawrence Berkeley National Laboratory
39 PUBLICATIONS 349 CITATIONS

[SEE PROFILE](#)



THE UNIVERSITY
of ADELAIDE

WHAT'S THE MATTER?
Supersymmetric Dark Matter Searches with CMS Data

Daniel T. Murnane

Supervisors: Dr. Martin White & Prof. Anthony G. Williams

A thesis submitted towards the degree of Honours in
Bachelor of Science in High Performance Computational Physics (Honours)

The Faculty of Sciences
The University of Adelaide

October 31, 2014

Acknowledgements

I hugely thank my supervisors,
my housemates, my parents
and, of course,
Natascha.

Contents

Contents	iii
1 Introduction	1
1.1 Dark Matter	1
1.2 A Super Theory	5
1.3 The Large Hadron Collider's Compact Muon Solenoid	6
1.3.1 Detector Layers	7
1.3.2 Parameters of an Experiment	8
1.4 The Project	10
2 Shadows of Supersymmetry	13
2.1 The Standard Model	13
2.1.1 Three Theories	13
2.1.2 $SU(3)$: Quantum Chromodynamics	14
2.1.3 $SU(2) \times U(1)$: Electroweak Theory	14
2.1.4 $SU(2)_W \times U(1)_Y \rightarrow U(1)_Q$: The Higgs Mechanism	15
2.1.5 The Unexplained	16
2.2 A Super Symmetry	17
2.2.1 R-Parity	18
2.2.2 Diary of a Wimpy Particle	19
2.2.3 Neutralino Mixing	20
2.3 SUSY in a Collider	21
2.3.1 The Collision	21
2.3.2 Observables	22
3 Computational Tools	25
3.1 The SUSY Les Houches Accords	25
3.2 Prospino	26
3.3 SoftSusy	26
3.4 Pythia	27
3.5 Delphes	27
3.6 Gambit	28
3.7 Root	28

4 Searching for Dark Matter at the LHC	29
4.1 Event Measurement & Simulation	29
4.1.1 Detector Triggers	30
4.1.2 Efficiency	30
4.1.3 Event Selection	31
4.1.4 Background Events	31
4.2 Signal Analysis Calibration	33
4.3 Running The Experiment	35
4.4 Likelihood Testing	38
4.4.1 Parameter Sampling	40
4.4.2 The Poisson Likelihood Function	40
4.4.3 Marginalisation	42
5 Numerical Results	43
6 Conclusion	49
Bibliography	51

1. Introduction

What does Supersymmetry mean in your life? It would be nice to offer a day-to-day example of the exotic Theory of Supersymmetry, but there simply isn't one yet. Instead, it might be that the best example is the very matter that holds our universe together. A majority of the matter in the universe doesn't interact strongly with what we think of as "ordinary matter" it is invisible, or "dark". Exhaustive tests have proven the existence of Dark Matter, and Supersymmetry has remained the best contender for its explanation. But in the 43 years since the inception of Supersymmetry, there has not been a single Supersymmetric particle observed. To guide and speed up this search, it is necessary to put limits on what such a particle could be. In this thesis, I perform this limit test on the particle most likely to be Dark Matter the neutralino. By modelling the physics of Supersymmetry with computational tools, signal predictions can be made and tested against data gathered at the Large Hadron Collider. The motivation for considering Supersymmetry is the explanation of this Dark Matter.

1.1 Dark Matter

That Dark Matter (DM) exists cannot be denied, but its particular properties remain to be explored. In this section, the evidence for DM will be presented. The many astrophysical experiments discovering this evidence will give us the constraints on DM required to test possible candidates in particle physics.

In 1932, Jan Oort noticed that stars in the Milky Way appeared to be moving fast enough to escape the galaxy. By comparing the light emitted from the stars with that emitted by the rest of the galaxy, he deduced their masses and velocity. Based on the measurements, there was no way the galaxy could maintain its structure. Oort concluded that if we assume that the galaxy is stable then there must be a great deal of "hidden mass", or dark matter.

Since those early days, there has been growing evidence of the existence of dark matter. Estimates now put the proportion of dark matter at 85.5% of the total matter of the universe. Almost all of the evidence comes from astrophysical observations of hidden mass. The classic example can be seen in a cluster of galaxies known as the Bullet Cluster. Two clusters made from hundreds of galaxies collided 150 million years ago. What we now think of as "ordinary"¹ matter in the form of stars passed through the collision mostly unaffected. The

¹Also very commonly called "baryonic" matter, though I find this confusing. The matter we see every day is mesonic, leptonic *and* baryonic

rest of the baryonic matter in the form of hot, intergalactic gas interacted electromagnetically and lost most of its velocity. There is nine times more gas matter than star matter, so most of the mass should be expected to be in the central, slowed region. But by observing the gravitational effects of the cluster, we see that most of the mass is hidden in the unaffected systems.

The two main forms of gravitational effects are gravity's effect on light - seen as gravitational lensing, and gravity's effect on mass - seen in galaxy rotation curves. The Bullet Cluster is an example of the first. Light from galaxies situated beyond the cluster must travel near the cluster's gravitational reach. As it does, it lenses - bending around the cluster. The huge collection of matter appears to us on Earth as a fishbowl held up to the night sky, distorting the stars. Jan Oort's observation is an example of the second effect.

Extremely precise measurements of spiral galaxies in the 1970s [1] developed Oort's work, showing the rotational velocities of stellar objects. Consider a simple model of a spherically symmetrical galaxy. The velocity of a star at radius R is given by Newton:

$$v^2 = \frac{GM(R)}{R}$$

Where M is the mass contained in a sphere with radius R . If the mass was distributed in the manner that is visible, one would expect the velocity to decrease as the red curve in Figure 1.1. However, observed velocities followed the green curve. Referring back to Newton's equation, for a flat velocity, one would require an enclosed mass that increased linearly as one receded from the galactic centre. This certainly doesn't agree with the luminous matter distribution, as in Figure 1.2.

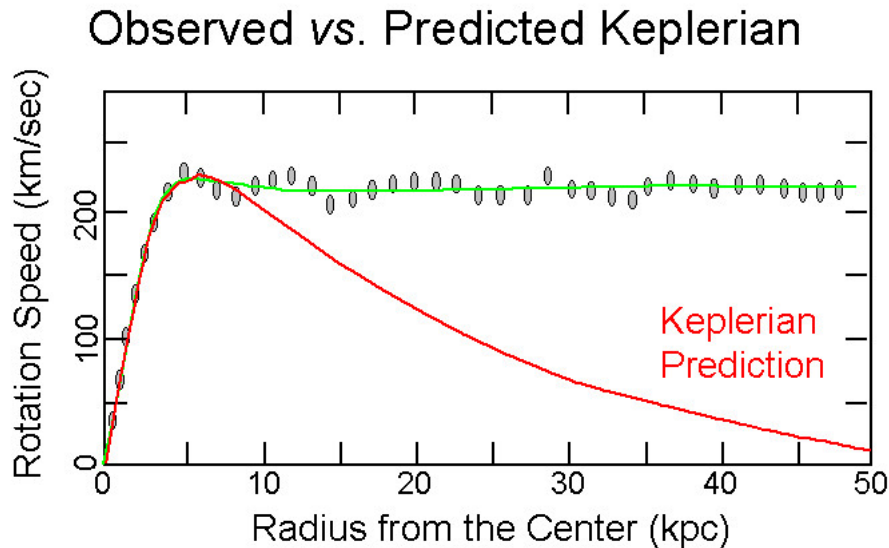


Figure 1.1: Observed vs. Keplerian-predicted orbits of a spiral galaxy.

One solution is to change the very nature of the stars' interactions. This is called Modified

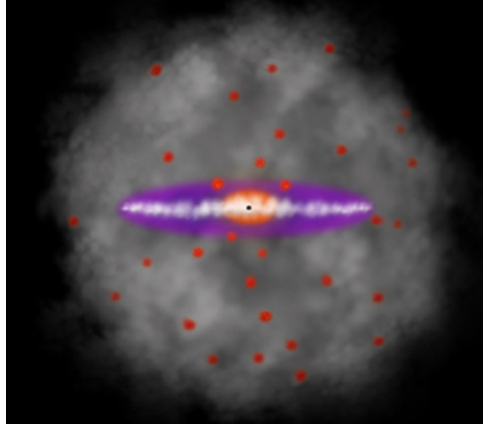


Figure 1.2: Luminous matter distribution of a spiral galaxy, permeated and surrounded by a “halo” of Dark Matter

Newtonian Dynamics (MOND). On the other hand, if we assume that the interactions are *not* altered, then an explanation is that the visible mass does not represent the total mass - that invisible matter is contributing significantly to the galaxy’s density profile.

The ratio of mass-to-light is denoted Υ . If all mass emitted light, then $\Upsilon = 1$. In the case of the Triangulum Galaxy, for example, $\Upsilon \approx \frac{1}{5}$ [2]. These ratios can be used to estimate a “relic abundance” - the density of DM thermally produced after the Big Bang, shortly before the period known as Baryogenesis.

Ordinary matter and dark matter is hypothesised to have decoupled after the order of the first 10^2 seconds. Prior to this, the universe had a density such that interactions occurred with $10^{16} \text{ GeV} \geq E \geq 10^3 \text{ GeV}$. At this energy, annihilation and creation occur in thermal equilibrium. The process that occurs next is very similar to a fractional distillation of moonshine - heating a mixture of various alcohols and cooling the boiled gas at the right temperature for drinkable ethanol to condense. For temperatures of $10^3 \text{ GeV} \geq E \geq 10^2 \text{ GeV}$, Dark Matter is theorised to have decoupled and condensed [3]. This matter has then been “Frozen Out” and begins the period of Structure Formation - the process of stellar objects forming galaxies, which form clusters. Only after Structure Formation had begun did ordinary matter condense at $E \leq 10^2 \text{ GeV}$. [4]

What does it mean to “see” matter? If Dark Matter is invisible, what exactly do we mean by “visible”? The usual convention is that visible matter must interact with light. In the Classical explanation, we would say that its material properties mean it either absorbs, reflects or refracts light. These are all situations visible to the naked eye, in the case of visible light (now it’s getting confusing! All radiation is visible if you have the right equipment, whether it’s an eye, an infrared camera, or a radio). In the Quantum explanation, visible matter must interact with photons. An electron is certainly visible as it can interact as:

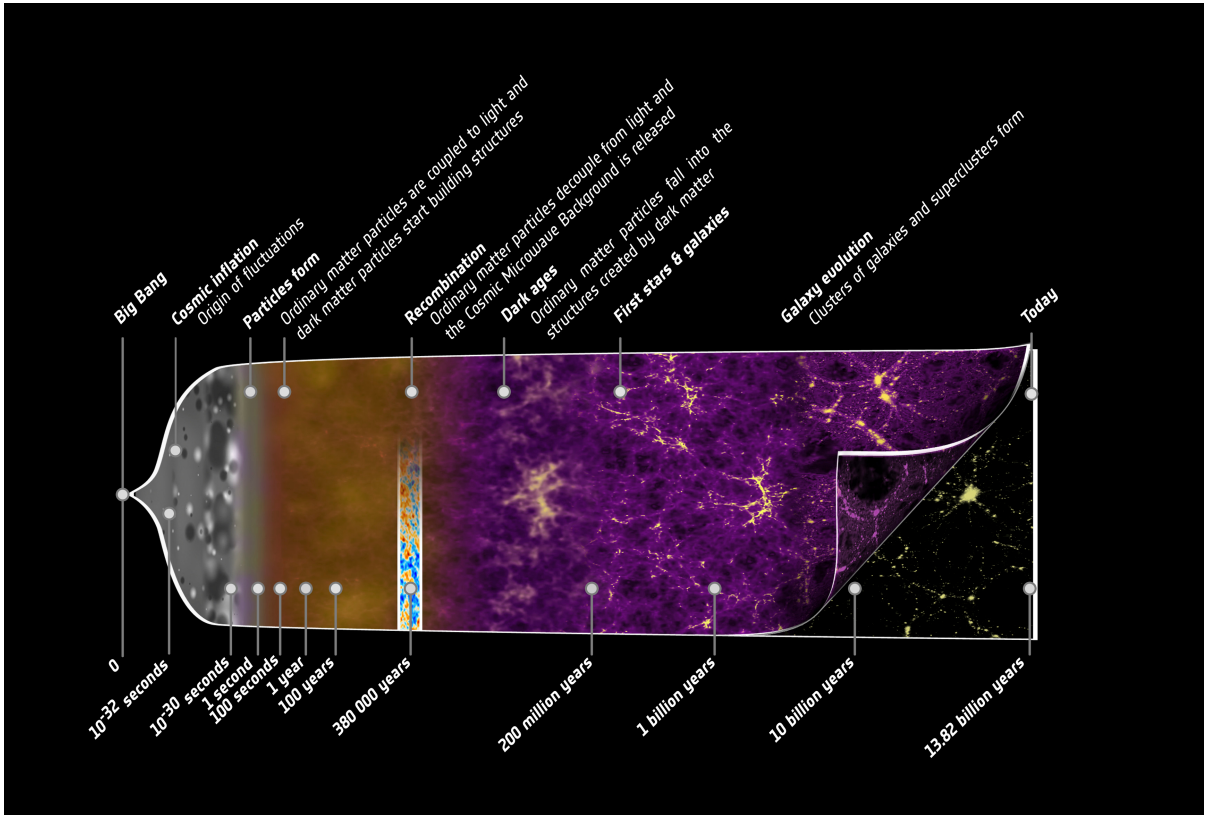


Figure 1.3: The theoretically and sexually suggestive model of Bottom-Up Structure Formation: Dark Matter freezes out after ~ 100 seconds

$$e^- + \gamma \rightarrow e^- + \gamma$$

In fact, almost every particle that we know of can absorb or emit photons in this way¹. This falls into the category of Quantum Electrodynamical interactions the medium strength interactions of particles. Thus, “seeing” particles in this way is quite easy. Easier than the Weak W/Z interactions, and easier to model than the Strong gluon interactions. “Invisible” must mean then a particle that doesn’t interact significantly with the electromagnetic field.

The evidence presented thus far puts some very specific constraints on how a dark matter particle might behave. We can deduce some of these constraints:

- The particle **cannot interact significantly with the electromagnetic field**. This follows from the period of Baryogenesis, when the collapse of ordinary matter produced the burst of radiation known as the Cosmic Microwave Background (CMB). The minimal fluctuations of the CMB put a limit on DM-photon interaction; between 10^{-6} and 10^{-4} the strength of an electron-photon interaction [5]. Similarly, the particle

¹The neutrino is the only confirmed particle not to interact electromagnetically. However, models proposing thermally-produced neutrinos as the sole source of dark matter fail to correctly predict relic abundance [4]

should not interact at all via the strong force, in order for DM to not interfere with Baryogenesis. DM may be self-interacting, however [6].

- The particle must be **gravitationally interactive**, in order to explain the spacetime curvature effects that have been observed. Given our knowledge of General Relativity, the particle must then have mass
- It must reproduce the observed statistics of **abundance**
- Assuming a particular particle is the dominant form of DM, it must be **stable** in order to explain the amount of DM remaining after the Big Bang

Astronomers have observed that 85.5% of the universe interacts normally with the gravitational field, but very weakly with the electromagnetic field. This simply doesn't fit any version of the current model of particle physics. Gravitational lensing, galactic rotation and the CMB provide the inescapable conclusion that mainstream physics is missing a form of matter, a form of interaction, or both.

1.2 A Super Theory

Having created a profile for a possible dark matter particle, let us change tack and consider a seemingly unrelated idea. In 1971 and 1972, three independent groups proposed a relationship, or symmetry, between the two fundamental species of matter - bosonic matter and fermionic matter. The theory required combining the highly successful Standard Model of particle physics with a set of spacetime transformations known as the Poincaré group. Together, the set of internal symmetries and spacetime symmetries makes up a theory of Supersymmetry (or "Susy"). In doing so, it resolves many outstanding flaws, or at least oversights, of the Standard Model. At present, the Standard Model is the most successful theory ever - it predicts the behaviour of, for example, electron interactions to one ten-billionth of a percent precision [7]. This is equivalent to predicting within 0.1 microseconds when the next Adelaide Metro bus will arrive (assuming Go-Zone calibration). However, problems with the Standard Model stem from its application at higher energies. There are unappealing implications when we try to measure SM physics at extremely small distances. For this reason, Beyond Standard Model (BSM) physics is generally thought to be a necessary endeavour for particle physicists and astrophysicists. Many BSM theories contain supersymmetry as a component.

This makes Susy an interesting and elegant theory in its own right. The mathematical tools produced to study Susy have gone on to be useful in many other fields, and it can be used in developing a so-called Grand Unified Theory that would include all the known forces. Its immediate importance to this thesis is the specific results of the Minimal Supersymmetric Standard Model (MSSM). This is the product of adding *only* the Poincaré symmetry to the Standard Model symmetries. In doing so, the number of particles in nature must be doubled.

Each Standard Model particle is assigned a "super-partner" with an opposing form of spin - each fermion is assigned a boson, and vice versa.

An important aspect of the MSSM is that the lightest Susy particle is guaranteed to be stable. Due to an internal symmetry of Susy particles, they can only be created or annihilated in pairs, and thus a solitary superpartner cannot decay. This lightest supersymmetric partner, or LSP, must have mass around the Weak scale for the theory to correctly solve the high-energy problems of the Standard Model. The MSSM can be extended to "constrained" models and, depending on these constraints, the set of particles most likely to have mass in the Weak scale are those particles called **gauginos** [8]. These are the superpartners of the Weak force gauge bosons. The subset called "neutralinos" do not interact electromagnetically and carry no colour charge. While Susy was not originally created to solve the astrophysical observations of Dark Matter, it provides an ideal Weakly Interacting Massive Particle. The criteria and properties are summarised in Figure 1.4.

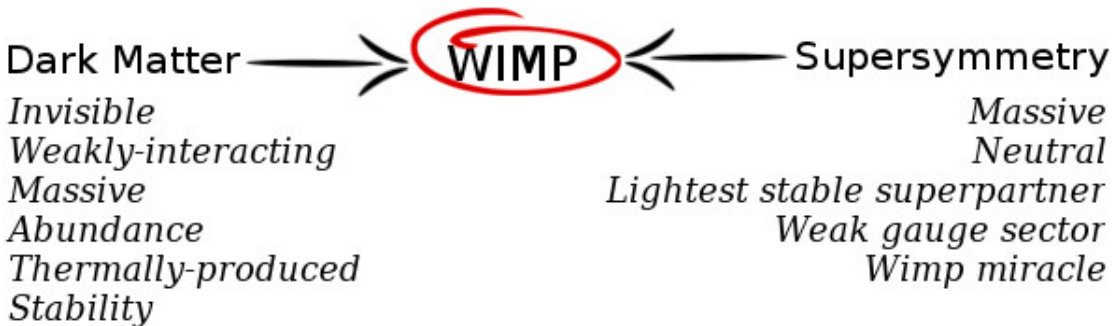


Figure 1.4: Properties of a WIMP

A particularly intriguing phenomenon is known as the **Wimp Miracle**. In only a few intuitive steps, one can deduce a rough estimate of the relic abundance of a Susy WIMP, with the assumptions of a Boltzmann distribution during the first few seconds of the universe, and a Weak-scale cross-section. To good approximation, this number agrees with the abundance of thermally produced DM.

However, while the characteristics of the theorised neutralino are well-described in the MSSM, its mass is taken as an independent parameter¹. The purpose of this thesis is to impose the limits on this mass that allow a physically possible model, given what we have observed at the Large Hadron Collider.

1.3 The Large Hadron Collider's Compact Muon Solenoid

Situated 175 metres below the Franco-Swiss border, the Large Hadron Collider is a 27 kilometre-long rollercoaster built for the sole enjoyment of protons. Two beams of protons

¹Actually, a function of four independent parameters, see Section 2.4

are accelerated in a circular tunnel and made to collide at four precise points - the detectors. The facility was opened in 2008, and by 2014 the collisions had a maximum energy of 8 Tera-electron-volts (TeV). Once it is fully operational, the collisions will occur at 14 TeV. This means that the protons will be travelling at 299.792455 kilometres per millisecond, a few ten-millionths of a percent slower than light. At this energy, extremely heavy and unstable particles can be formed from the quarks interacting within two colliding protons. It is therefore an ideal environment to look for particles such as the Higgs Boson, and supersymmetric partners.

In fact, *two* detectors were built to search for these particles - A Toroidal LHC Apparatus (ATLAS) and the Compact Muon Solenoid (CMS). Each have had exciting discoveries since 2008, and complemented the research of the other.

1.3.1 Detector Layers

The CMS collaboration have produced comprehensive studies of processes that might involve supersymmetric partners. A cut-away design of the detector is seen in Figure 1.6.

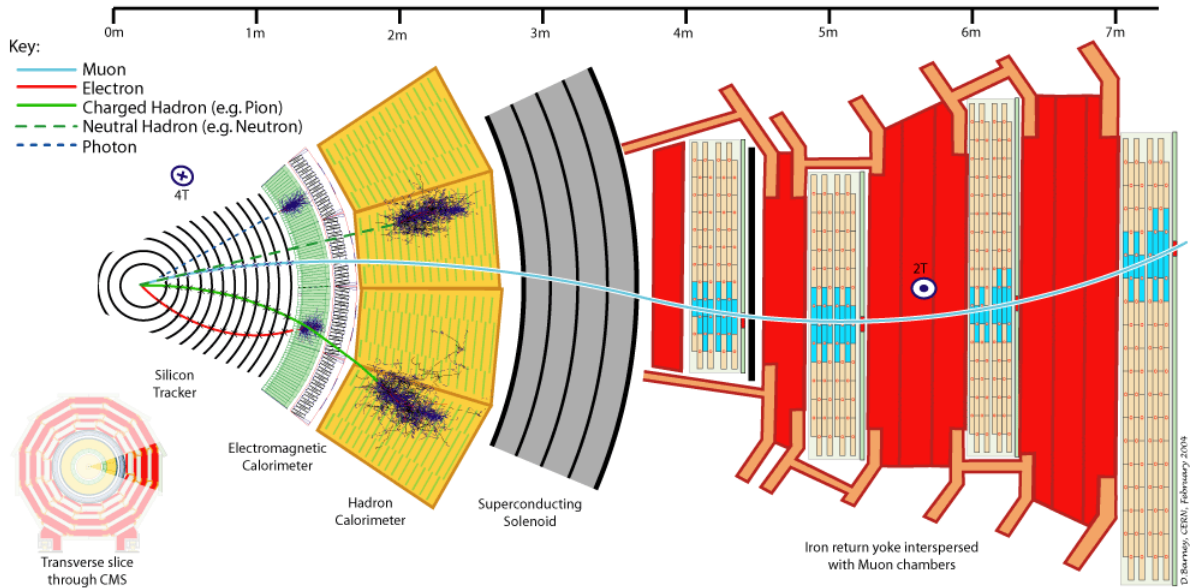


Figure 1.5: The calorimeters of each layer in the CMS detector

Brief description of the design and geometry of CMS

The detector is designed to work in layers. Each layer of the detector's onion construction detects a different type of particle. The order of each layer is chosen so as to absorb the most interactive particles first. The layer schematic is shown in Figure 1.5. From innermost to outermost we can see:

- **Tracker:** In order to obtain a full picture of each particle before it is absorbed in its particular detector, it is necessary to measure its initial trajectory. The Tracker consists of a shoebox-sized set of 60 million silicon pixels. These pixels are extremely sensitive and interact very lightly with the particles being measured, so the three-momentum can be found without affecting the particle's final energy. They are surrounded by a tennis-court-worth of silicon strips. The inner tracker is bombarded by 10 million particles per centimeter per second. It is able to detect and reconstruct the path of each of these particles.
- **The Electromagnetic Calorimeter - ECAL:** Photons and electrons interact with electrically charged particles. The first layer of the detector is designed to be particularly sensitive to these particles. When they pass through the ECAL, the transparent pixels scintillate and release light. Photodiodes attached to each pixel pick up this light, which can be used to calculate the energy deposited at that point. The sum of each scintillation gives the particle's initial kinetic energy.
- **The Hadronic Calorimeter - HCAL:** The next layer is built to detect hadrons - baryons and mesons consisting of quarks and gluons. It consists of alternating plates of absorbing material and detecting material. The detectors are scintillators, as in the ECAL. The absorbers are thick metals that cause the hadrons to split and form jets. Further discussion of jets is found in Section 2.4.
- **Magnetic Layer:** A supercooled superconducting electromagnet produces a 3.8 Tesla magnetic field. It is this field that allows the charge of particles to be measured in the other layers. The amount of curvature traced out is directly proportional to the particle's momentum and charge, and the magnetic field strength.
- **Muon Detectors:** A muon is from the lepton family, along with the electron, but 200 times more massive. This momentum carries the muon through many of the more inner absorbers. The speed of the muon relativistically lengthens its lifetime, so specialty detectors are placed around the CMS magnet to catch these elusive particles.

1.3.2 Parameters of an Experiment

With an idea of the detector's geometry, it is import to review some concepts and quantities present in the equipment. The *luminosity* \mathcal{L} of the Large Hadron Collider is the number of protons that could collide per centimeter per second. The number we will use later in the thesis is the *integrated* luminosity L :

$$L = \int dt \mathcal{L}$$

The integration is taken over the time that collisions have been performed at a particular energy, and represents the total number of collisions that *could have* occurred, per centimeter.

The value is closely related to the cross-section, with units given in the inverse of the cross-section.

1.4 The Project

Dark Matter is an important gap in scientific knowledge, and Supersymmetry may fill in some of this gap. For my honours project, I have taken the most general form of the Minimal Supersymmetric Standard Model and searched for the most likely processes to produce Dark Matter - the neutralinos. Based on these simulations, we can say whether these particles are disproven by current CMS measurements, or whether they could still have mass at these energy levels, in spite of not being measured.

The first task in this thesis is to explore in an accessible way the concepts of Supersymmetry that are useful in the search for Dark Matter. In Chapter 2, a brief study of the current Standard Model and its shortcomings will help motivate its generalisation to Supersymmetry. The second task is to introduce the many computational tools used in the search - these are the equipment of the quasi-experiment. They allow the formidable mathematics of Supersymmetry to be applied in randomly-generated simulations. Indeed, the third task is to describe the numerical predictions of Supersymmetry and explore how closely they reflect reality. In Chapter 4, the reason and method behind Dark Matter mass scans are explained. The project concludes with analysis of the numerical results. We can calculate likelihoods of each of the supersymmetrical models being correct. All of these likelihoods will give “exclusion limits” - limits on the mass of Dark Matter particles given what we have found in the Large Hadron Collider. These limits may give a guide on where to look next for Dark Matter, when the LHC starts operating again in 2015.

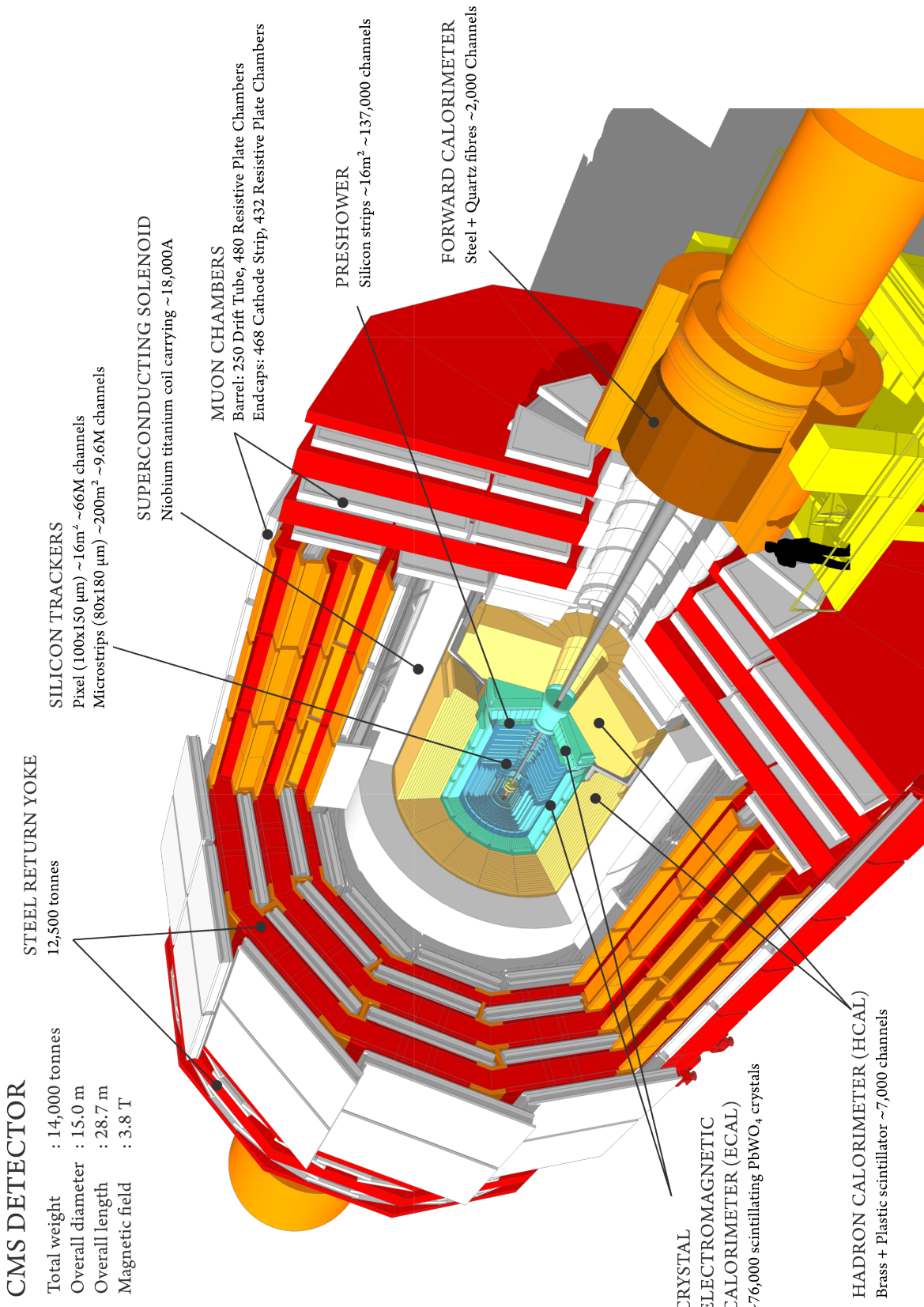


Figure 1.6: Design of the CMS detector

2. Shadows of Supersymmetry

Given now that we have a reason to care about Supersymmetry, how do we find out if it's true, or even possible? The following is a very brief overview of what Supersymmetry qualitatively predicts, how to test those predictions, and why the gauginos are the particle of choice in the search for dark matter.

DISCLAIMER: The following is a discussion of the MSSM, an R-parity-conserving, least-possible-extension to the SM.

2.1 The Standard Model

2.1.1 Three Theories

The Standard Model (SM) is actually a collection of three independent theories, two of which have been successfully unified into one. They all happen to follow the same procedure - gauge invariance. There are gauges, or degrees of freedom, which can be changed without altering the physics it describes. Together, they comprise the most accurate physical model ever created. They describe all the known particles and forces, except for gravity sadly. The three gauge symmetries have a group structure, and can be written:

$$SU(3) \times SU(2) \times U(1)$$

In the following sections, each of these symmetries shall be reviewed (based heavily on [9]).

All the SM matter particles are called fermions - they have spin $\frac{1}{2}$. The spin has several important implications. Spin $\frac{1}{2}$ particles can have anti-particles, no two can exist in the same quantum state, and they behave according to Fermi-Dirac statistics. The SM *force* particles, on the other hand, are called bosons. They "mediate" the three SM forces. In classical mechanics, a particle experiences a force. In quantum field theory (QFT), a particle interacts with a force-mediating particle. The SM bosons have spin 1 and behave according to Bose-Einstein statistics. There are 24 SM particles in total, as can be seen in Figure 2.1. Each of these particles is governed by one or more of the above symmetries.

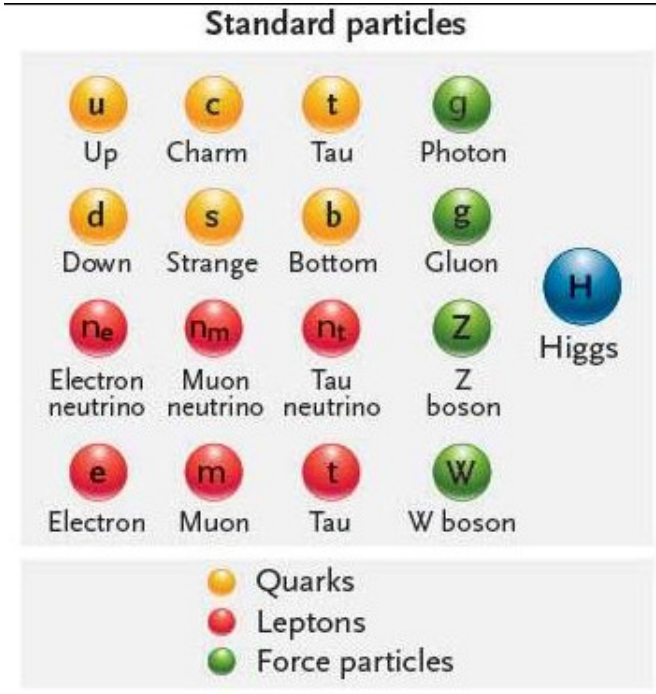


Figure 2.1: The particles described in the Standard Model

2.1.2 $SU(3)$: Quantum Chromodynamics

The QCD group $SU(3)_{\text{colour}}$ prescribes how particles transform under coloured interactions. Only the six quarks and eight massless gluons experience this “coloured” force, known as the strong force. The strong force is so named as it holds quarks together within protons, neutrons, and other baryons and mesons. No quark has been observed to have escaped the strong force to become an isolated particle; this is the principle of Confinement. The colour charge of a quark or gluon - combinations of red, blue and green - determines how it interacts with other quarks and gluons.

2.1.3 $SU(2) \times U(1)$: Electroweak Theory

The group $SU(2)_{\text{isospin}} \times U(1)_{\text{hypercharge}}$ prescribes how particles transform under electroweak interactions. As in QCD, forces are mediated by massless gauge bosons, known as W^1 , W^2 , W^3 and B bosons. The nature of their interaction with a matter field ψ is given by the covariant derivative:

$$D_\mu \psi = \partial_\mu \psi - ig W_\mu \cdot \frac{\vec{\tau}}{2} \psi - ig' Y B_\mu \psi$$

Where τ are the Pauli matrices, and Y is a diagonal “hypercharge” matrix. When this is expanded out, we see terms like $g(W_\mu^1 - iW_\mu^2)$ and $g(W_\mu^1 + iW_\mu^2)$ from the Pauli matrices. As the terms within the parentheses have the same coupling strength and quantum numbers,

they must together describe a single particle. These *physical* particles are called $W_\mu^\pm = \frac{1}{\sqrt{2}}(W_\mu^1 \mp iW_\mu^2)$. Similarly, we get terms suggesting two more physical particles, denoted

$$Z_\mu = \frac{-g'B_\mu + gW_\mu^3}{\sqrt{g^2 + g'^2}}$$

and

$$A_\mu^\gamma = \frac{gB_\mu + g'W_\mu^3}{\sqrt{g^2 + g'^2}}$$

This is a process known as “mixing” - linear combinations of particles in a gauge-invariant basis producing physical particles in the mass-eigenstate basis. Mixing is an extremely important phenomenon that will be used later to find the mass of supersymmetric particles.

While the W_μ^\pm, Z_μ are now in the mass-eigenstate basis, their mass terms go to zero. Only after they couple to the Higgs particle will they have non-zero mass.

2.1.4 $SU(2)_W \times U(1)_Y \rightarrow U(1)_Q$: The Higgs Mechanism

In QFT, a particle is considered an excitation of a field. Just like a stretched sheet of rubber being flicked, a particle oscillates like a spring in its field with a potential energy of

$$V \sim |\Phi|^2$$

with $|\Phi|$ being the amplitude of the excitation. However, in the Higgs Mechanism we propose a particle with a potential

$$V \sim \mu^2(|\Phi|^2 - v^2)^2$$

That is, even with $|\Phi| = 0$, there is a non-zero vacuum expectation value (vev) of μ^2v^2 . This is not physically realistic, though it still preserves the gauge symmetry of the Electroweak group. To be physical, this Higgs particle should spontaneously collapse to a true minimum at $|\Phi|^2 = v^2$. In doing so, it breaks the symmetry $SU(2) \times U(1)$.

The previously massless W_μ^\pm, Z_μ bosons interact with the Higgs and acquire mass terms proportional to v^2 . It is then useful to parameterise the combination of gauge bosons with a value called the Weinberg angle, θ_W . Expressing the mixture as

$$\begin{aligned} Z_\mu &= \cos \theta_W W_\mu^3 - \sin \theta_W B_\mu \\ A_\mu^\gamma &= \sin \theta_W W_\mu^3 + \cos \theta_W B_\mu \end{aligned}$$

gives a relation for the gauge boson masses:

$$\frac{m_W^2}{m_Z^2} = \cos^2 \theta_W$$

and the Higgs mass:

$$m_H^2 = 4\mu^2 v^2$$

2.1.5 The Unexplained

One of the breakthrough suggestions from the Standard Model is that there is no such thing as a “bare”, or isolated particle. When an electron interacts with a photon, loop corrections occur; the creation and annihilation of virtual particles. These loop corrections “dress” the bare particle and give it an observable mass that is proportional to the strength of the loop interactions.

As noted above, the Higgs Boson gives mass to electroweakly interacting particles proportional to the interaction strength λ_f and therefore the mass of the Higgs itself, as in 2.2. In the case of a top quark, the heaviest SM particle, the loop correction is relatively enormous. Specifically, the first order, most divergent correction is

$$\Delta m_H^2|_{f=\text{top quark}} = -\frac{|\lambda_f|^2}{8\pi^2} \Lambda_{\text{Planck}}^2|_{f=\text{top quark}} \sim 10^{38} \text{ GeV}^2$$

Λ is a constant that cuts off the correction above some arbitrary energy. I have chosen the Planck scale as an example of where the Standard Model is hugely divergent. There is nothing inherently wrong with this, but the dressed mass of the Higgs Boson has been *measured* to be 125.03 GeV. Somewhere we must find a constant that brings the divergence back to the electroweak scale. The only available constant is λ_f , which must be fine-tuned by 38 orders of magnitude. This seems unnatural, and it’s preferable to find a more fundamental, elegant solution.

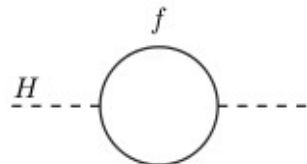


Figure 2.2: A coupling of Higgs and fermion. The mass of the Higgs is corrected by such interactions

The Standard Model does not fail at high energies, but it requires fine tuning. As with the particle mass corrections, the coupling “constants” are also corrected as we move to more energetic physics. The running of these constants is seen in figure 2.3.

Again, there is no inherent reason that the couplings need converge. However, it seems supremely unnatural that they should run to almost the same value, but not converge in some grander, unified theory. The Almighty would be having a mighty joke if the Standard Model really was the last word on this convergence.

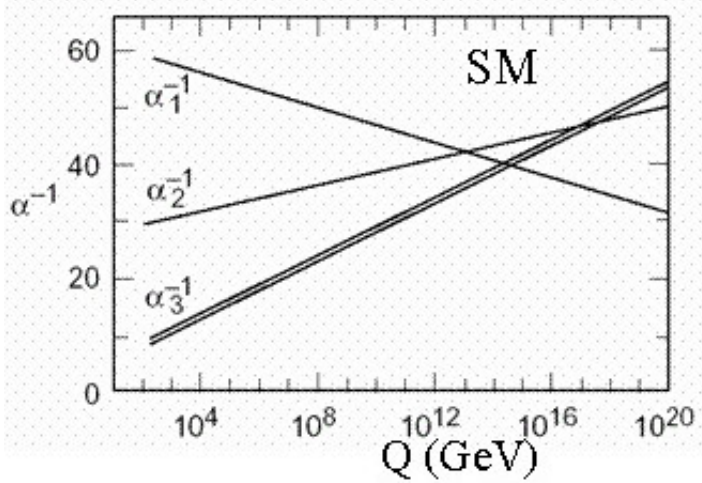


Figure 2.3: The running of SM coupling constants is not convergent at high energies

2.2 A Super Symmetry

As mentioned in the Introduction, the theory of Supersymmetry provides a way of solving the Dark Matter conundrum. But adding an extra symmetry to the Standard Model also resolves some of the unexplained phenomena in the model. While the Standard Model follows the dynamics of quantum field theory and is therefore compatible with relativity, merging its gauge transformations with spacetime transformations in the usual Lie Algebra procedure proved impossible. Only once the concept of extending these algebra to a *graded* Lie Algebra could the two sets of symmetries produce (anti)commutation relations. A graded 2-algebra discriminates between even and odd operations. Then we can introduce an operator \hat{Q} that acts according to a commutative or anti-commutative Lie algebra, depending on whether it is applied to a fermion or boson. In doing so, it switches the spin state of this particle:

$$\begin{aligned}\hat{Q}(\text{fermion}) &= \text{boson} \\ \hat{Q}(\text{boson}) &= \text{fermion}\end{aligned}$$

The transformed state is the particle's superpartner. The Standard Model contains twelve bosons and twelve fermions (and a Higgs boson); it might have been that each had a superpartner within the SM. As it is, this is impossible for *any* of the SM particles. A particle and its superpartner must exist in a supermultiplet that shares quantum numbers, and transform as the conjugate of each other. This is not the case for any SM fermion-boson pair. Thus, we introduce another set of 25 particles, known as sparticles. These are listed in Figure 2.4. Each quark and lepton is assigned a squark and slepton. The gluons and photon are assigned gluinos and a photino. The Higgs boson is assigned a Higgsino. Finally, the gauge bosons in the unbroken Electroweak groups are assigned gauginos.

If supersymmetry were an “exact symmetry” (i.e. there were no cop-outs) then an electron and selectron would be identical save for their spin. As it stands, no selectron has ever been

Standard particles				Supersymmetry particles			
u Up	c Charm	t Tau	g Photon	~u Squark	~c Slepton	~t Neutralino & Chargino	~g Photino
d Down	s Strange	b Bottom	g Gluon	~d Squark	~s Slepton	~b Neutralino & Chargino	~g Gluino
ne Electron neutrino	nm Muon neutrino	nt Tau neutrino	Z Z boson	~ne Slepton	~nm Neutralino & Chargino	~nt Neutralino & Chargino	~Z Zino
e Electron	m Muon	t Tau	W W boson	~e Slepton	~m Neutralino & Chargino	~t Neutralino & Chargino	~W Wino
Quarks		Leptons		Neutralinos & Charginos			

Figure 2.4: The table of particles appearing in the Minimal Supersymmetric Standard Model

measured in an experiment, and a heck of a lot of electrons have been measured. It must be that for Susy to be possible, the selectron and all the other sparticles have been too heavy (i.e. too energetic) to be measured thus far. The heavier a particle it is, the faster it decays in general. It may be that these heavy particles will decay too quickly for them to make up 85% of the matter in our universe. Luckily, there is a prediction by the MSSM that saves some supersymmetric particles from decaying to ordinary matter.

2.2.1 R-Parity

The Standard Model has many quantities that are conserved - energy, charge, and lepton and baryon numbers. The latter two are explained by quark and electroweak symmetries, but should still be conserved when we extend the SM to Susy. If they are violated in Susy, the proton is able to decay in as little as 10^{-2} [10] seconds; not a good prediction given a proton has never experimentally decayed. To build a theory without proton decay, we must enforce an extra conservation called R-parity.

As in normal parity, which has the options of left and right, R-parity has only two elements. The options are R-positive or R-negative, given by:

$$P_R = (-1)^{3B+L+2s}$$

where B is the Baryon number, L is the Lepton number, and s is the total spin.

It appears that in order to obey R-parity, particles can only be created or destroyed in pairs. Just as, in order to conserve charge, an electron and positron can annihilate to produce a

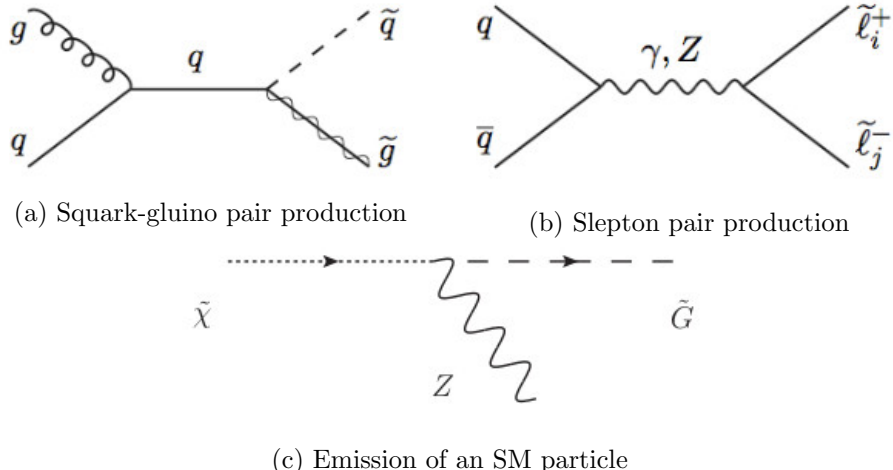


Figure 2.5: R-Parity conserving processes

charge-less photon, particles with opposite R-parity can annihilate. For example, consider the Susy processes in figure 2.5.

Each of these particles have R-parity= \pm , which is conserved in the final state. However, the third process has an exception. The final particle must have a mass less than the initial particle. But what if these are the lightest Susy particles, and that they could never give an even R-number. What I'm really asking is: What if supersymmetry predicted a new particle that couldn't decay to ordinary matter, that was relatively light and neutral? The answer is: It does, and this particle is therefore a perfect candidate for Dark Matter.

2.2.2 Diary of a Wimpy Particle

Recall the discussion of seeing matter in the introduction. In order for Dark Matter to be dark, it must interact weakly (that is, not considerably the interaction may be Electromagnetic, Weak or Strong). But it must also be massive in order to produce the observed gravitational effects. Such a particle is called a WIMP, a Weakly Interacting Massive Particle. R-Parity guarantees that there exists at least one stable supersymmetric particle. It's possible that this isn't the source of dark matter at all, that there exist both a stable Susy partner and heavier dark matter particles that are not at all related. But it very tempting to suggest they are the same.

We can analyse the Susy family for a WIMP-candidate, and thus propose this particle as the LSP. The gauginos are particles that interact weakly. We should ignore the charginos, as they interact electromagnetically, and concentrate on the neutralinos. The neutralinos $\tilde{\chi}_1^0, \tilde{\chi}_2^0, \tilde{\chi}_3^0, \tilde{\chi}_4^0$ exist as an admixture of three superpartners to the SM gauge bosons: $\tilde{Z}, \tilde{A}, \tilde{H}$. We define $m_{\tilde{\chi}_1^0} < m_{\tilde{\chi}_2^0} < \dots$. Our model then requires that one of these states is the lightest supersymmetric partner. We should get to know the neutralino a little better, as it is the



Figure 2.6: Three vertices of gauginos: gaugino \rightarrow gaugino + gauge boson, gaugino \rightarrow antifermion + scalar, and antigaugino \rightarrow fermion + complex-conjugate scalar

main character of this thesis. It's most important interaction vertices are in figure 2.6[10].

The physical particles interacting here are in the mass-eigenstate basis. Not unlike the gauge bosons from the Standard Model, we must first find an appropriate expression to diagonalise the covariant derivative.

2.2.3 Neutralino Mixing

In the supersymmetric Lagrangian, the neutralino supermultiplet is not in a mass-eigenstate basis $\{\tilde{\chi}_1^0, \tilde{\chi}_2^0, \tilde{\chi}_3^0, \tilde{\chi}_4^0\}$. Instead, we have the fields:

$$\mathcal{L}_{\chi_m} = -\frac{1}{2}(\psi^0)^\top M_{\tilde{\chi}} \psi^0$$

This is because it exists in a unified Supersymmetrical version of the electroweak particles. In the Standard Model, the photon and gauge bosons were successfully explained in a single Electroweak theory. This requires expressing them as linear combinations of W and B bosons, which are not physical particles, but mathematical particles. Similarly, when extending the SM to MSSM, the neutralinos and gauginos are combinations of Winos, Bino, and Higgsinos: mathematical particles. It's these particles that are explicitly included in the SUSY Lagrangian. To find out how the neutralinos interact, we first need to break the SUSY Lagrangian with the Higgs mechanism, to see that the Bino and neutral Wino become a Zino and photino. The next step is to find out how precisely the Winos, Zino, photino and Higgsinos mix together. The nature of the mixing is given in the symmetric neutralino Mixing Matrix.

$$M_{\tilde{\chi}} = \begin{pmatrix} M_1 & 0 & -\cos \beta \sin \theta_W m_Z & -\sin \beta \sin \theta_W m_Z \\ M_2 & \cos \beta \cos \theta_W m_Z & -\sin \beta \cos \theta_W m_Z & 0 \\ 0 & 0 & -\mu & 0 \end{pmatrix}$$

θ_W is the Weinberg angle defined in the previous subsection. We also introduce the four new parameters here. We can find a unitary matrix U such that

$$\tilde{\chi}_i = N_{ij} \psi_j^0$$

$$\implies N^* M_{\tilde{\chi}} N^{-1} = \begin{pmatrix} m_{\tilde{\chi}_1} & 0 & 0 & 0 \\ 0 & m_{\tilde{\chi}_2} & 0 & 0 \\ 0 & 0 & m_{\tilde{\chi}_3} & 0 \\ 0 & 0 & 0 & m_{\tilde{\chi}_4} \end{pmatrix}$$

The matrix converts the set of Zino, photino, Higgsino into real, measurable, physical particles. Elements of the matrix are written in terms of the parameters M_1 , M_2 , μ and β . Note that a tan is usually taken of the fourth parameter: $\tan \beta$, as this is how it enters the matrix. The more diagonal this matrix is, the more $\tilde{\chi}_1^0$ is “Bino-like”, $\tilde{\chi}_2^0$ “Wino-like” and $\tilde{\chi}_3^0$ and $\tilde{\chi}_4^0$ “Higgsino-like”. Once we propose a particular M_1 , M_2 , μ and $\tan \beta$, we are in a position to start testing the mass of the proposed LSP.

2.3 SUSY in a Collider

2.3.1 The Collision

Unlike measuring the weight of an apple, the search for a neutralino is complicated by two issues. The first is that all SUSY particles including the neutralino may be extremely heavy. There is no upper bound (except at the point where quantum gravity is relevant) to their mass. They may be too energetic to be created in a 21st-century collider. The second is that even if they were to be created, the neutralino is dark. It doesn't interact significantly with ordinary matter, so is invisible for all intents and purposes. Of the former, we can use this absence of signal as a way to constrain the masses of neutralinos. If they are not measured, then they simply must be a higher mass than available at the LHC. This may seem like a cop-out. But this is not absence of evidence, it is evidence of absence. We can then say with certainty what a neutralino is *not*, and this is often just as useful in model-building as the more positive version. Of the latter, we can use the invisibility in a positive way. To see this, consider a process that is tested in this thesis, in figure 2.7.

While the neutralinos will escape without detection, the leptons will certainly be detected. Moreover, we know accurately the rate at which the SM allows lepton production. The particular final state above is called a “tri-lepton signature” or signal. Consider colliding protons a hundred thousand times, and the SM predicting ten of those will have tri-lepton final states. If we measure fifteen, and five of those have significant missing energy, then we may have indirectly observed five processes with BSM physics.

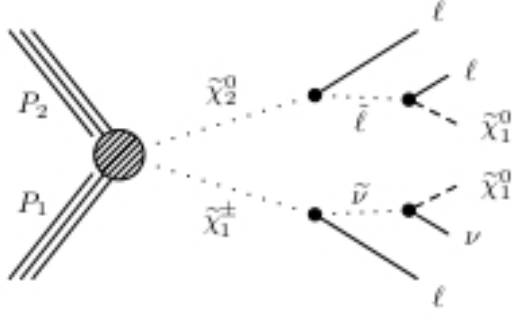


Figure 2.7: A trilepton final state indicating a possible supersymmetric process

For the purposes of this project, the measured value has already been established at the LHC. These are the “observed” events. The ten SM-predicted events are the “background”, and the five BSM-predicted events are the “signal” events. The more consistently the number of (background + signal) events replicate the number of observed events, the more likely the proposed BSM theory is. To disentangle signal events from the slew of other interactions occurring, there are several important values that characterise the process.

2.3.2 Observables

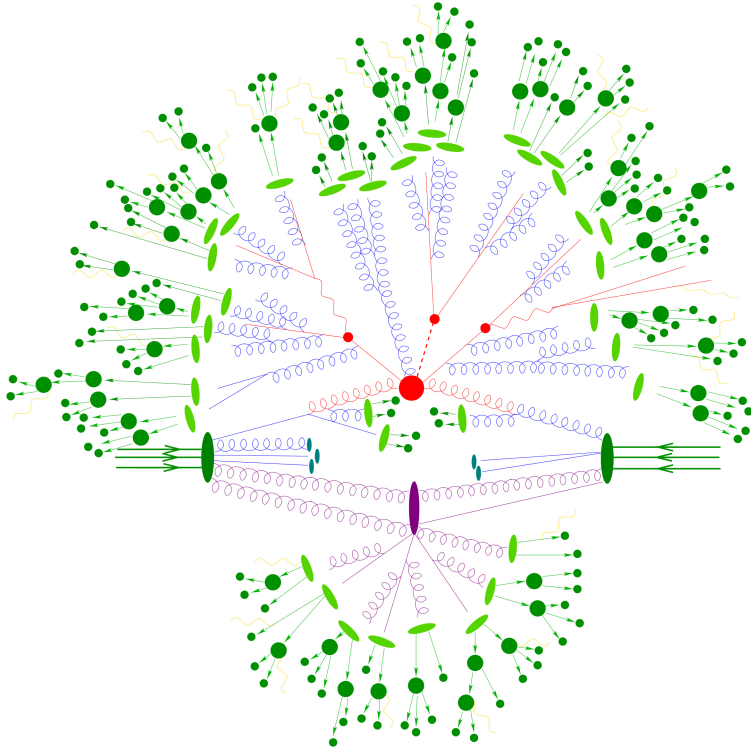


Figure 2.8: A typical CMS event - proton-proton collision produces isolated leptons, hadrons and jets

Consider again figure 2.7. Let’s go into more detail on this particular process:

$$P + P - > 3l + \nu + 2\tilde{\chi}_1^0$$

It is an electroweak process, so the signal will not be as great as the strong processes producing gluons and jets. The greater the mass difference between the $\tilde{\chi}_1^\pm$ and $\tilde{\chi}_1^0$, and the $\tilde{\chi}^0$ and $\tilde{\chi}^1$, the greater the energy of lepton production. In order to measure this energy, we need a trustworthy observable. The total momentum is not useful, as can be seen in figures 2.8 and 2.9. The proton is a composite object, and so it cannot be determined which momentum along the beampipe, p_z , is attributed to which process. The momentum perpendicular to the beampipe must be initially zero. So the **transverse momentum** p_T of each particle must sum to zero, and this gives an indication of invisible products:

$$E_T^{\text{miss}} = |\vec{E}^{\text{miss}}| = \left| - \sum_i p_T(i) \right|$$

where \vec{E}^{miss} is the missing transverse momentum vector.

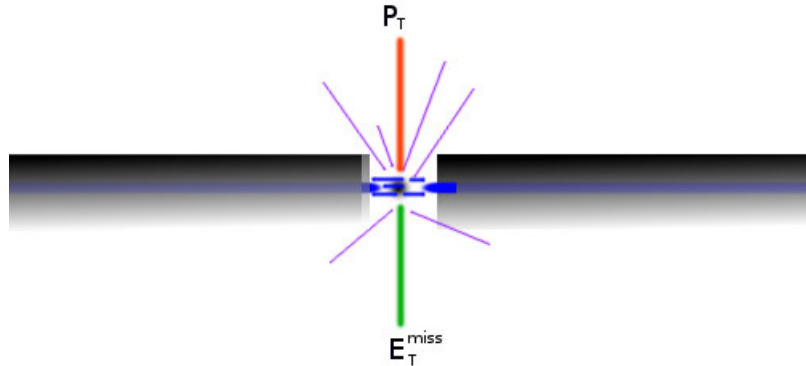


Figure 2.9: The transverse momentum summed must be the negative of the missing energy

The **transverse mass** and **invariant mass** are conceptually similar to the transverse momentum and, indeed, to each other. The transverse mass is generally given by [11]:

$$\begin{aligned} M_T^2 &= E_T^2 - \vec{p}_T^2 \\ &= \{E_T(1) + E_T(2)\}^2 - \{\vec{p}_T(1) + \vec{p}_T(2)\}^2 \\ &= m_1^2 + m_2^2 + 2\{E_T(1)E_T(2) - \vec{p}_T(1) \cdot \vec{p}_T(2)\} \end{aligned}$$

If we take one of the momenta to be the missing energy, and the other to be from a massless particle (e.g. a lepton and a neutralino, as we do in Chapter 4)¹ then the formula simplifies to

$$M_T = \sqrt{2E_T^{\text{miss}}|\vec{p}_T|(1 - \cos \phi)}$$

where ϕ is the angle between the two momenta. The invariant mass is simply the mass of an object at rest, and can be calculated by using the above, and not restricting to transverse

¹The lepton has non-zero mass, but it is far below the electroweak scale. When squared, it is negligible compared with the missing energy of a neutralino

components.

In practice, the invariant mass is used with neither missing energy nor massless particles. It is often possible to predict the mother of two detected particles. The mass corresponding to the sum of their momenta is the invariant mass of their mother, and can then be used to reconstruct the event. Examples are given in subsection 4.1.4.

3. Computational Tools

You are playing blackjack in the oldest casino in Monaco, the Monte Carlo. The automated card shuffler holds 8 decks, so we can be sure that the cards dealt are pseudorandom (not *perfectly* random, but very close). You bet the €25 minimum and hit appropriately, winning the hand. You have just run a simulation, that is, a simple event with a known set of rules that produces a definite output. In this case, there are enough rules to calculate the odds of winning a particular hand. This is the “analytical” solution. It requires sitting down with a sheet of paper and performing a great deal of algebra. For blackjack, the analytical solution is 42.22% chance of a win.

There is another type of solution. It requires letting all the players in the casino place their bets and letting all the card shufflers produce random wins and losses. We monitor the number of winners and losers, and eventually this overall proportion will start to mirror the true, analytical solution of 42.22%. We have then used numerous simulations to arrive at a “numerical” solution, specifically using the eponymous Monte Carlo Method.

To complete the metaphor, Supersymmetry is the largest, most complicated game of blackjack ever played. One where not even all the cards are known. We simply don’t know enough rules to produce an analytical solution, but we can use Monte Carlo simulations to approximate the solution. The computational devices used to simulate a SUSY process in the LHC are built to mirror reality. There is parameter randomisation, a simulated collision chamber and a simulated detector. The following explains each piece of equipment in the simulation. Their specific combination for this project is detailed in Chapter 4.

3.1 The SUSY Les Houches Accords

A particularly unforgiving aspect of SUSY is that it contains over 100 independent parameters. In order to feed these into a simulation, it is necessary that all physicists agree on what they’re talking about. This agreement is called the Supersymmetry Les Houches Accord (SLHA). Held in 2004 in Les Houches, France, the accord lists the Supersymmetry parameter names and the format of files containing these parameters, among many other things. With the universal labels agreed upon, SLHA files can be generated that can feed into many different simulators [12]. For example, figure 3.1 shows an SLHA file used in this project.

```

# SOFTSUSY3.5.0 SLHA compliant output
# B.C. Allanach, Comput. Phys. Commun. 143 (2002) 305-331,
Block SPINFO          # Program information
  1  SOFTSUSY      # spectrum calculator
  2  3.5.0        # version number
Block MODSEL # Select model
  1  0        # nonUniversal
Block SMINPUTS       # Standard Model inputs
  1  1.27934000e+02  # alpha_em^(-1)(MZ) SM MSbar
  2  1.16637000e-05  # G_Fermi
  3  1.17200000e-01  # alpha_s(MZ)MSbar
  4  9.11876000e+01  # MZ(pole)
  5  4.25000000e+00  # mb(mb)
  6  1.73300000e+02  # Mtop(pole)
  7  1.77700000e+00  # Mtau(pole)
Block MINPAR         # SUSY breaking input parameters
  3  1.98947000e+01  # tanb, DRbar, Feynman gauge
Block EXTPAR         # non-universal SUSY breaking parameters
  0  -1.00000000e+00  # Set MX=MSUSY
  1  1.02795000e+02  # M_1(MX)
  2  3.35860000e+02  # M_2(MX)
  3  4.50000000e+03  # M_3(MX)
  11 0.00000000e+00  # At(MX)
  12 0.00000000e+00  # Ab(MX)
  13 0.00000000e+00  # Atau(MX)
# SOFTSUSY-specific non SLHA information:
# MIXING=0 Desired accuracy=1.00000000e-03 Achieved=1.00000000e-03
Block MASS            # Mass spectrum
  # PDG code   mass           particle
    24  8.03828238e+01  # MW
    25  1.24001381e+02  # h0
    35  4.50000901e+03  # H0
    36  4.49999986e+03  # A0
    37  4.50109202e+03  # H+
  1000021  4.75055705e+03  # ~g
  1000022  9.87317353e+01  # ~neutralino(1)
  1000023  2.71244775e+02  # ~neutralino(2)
  1000024  2.70304584e+02  # ~chargino(1)
  1000025  -3.07725285e+02  # ~neutralino(3)
  1000035  4.02250355e+02  # ~neutralino(4)
  1000037  4.02566621e+02  # ~chargino(2)
  1000001  4.65444204e+03  # ~d_L
Block nmix            # neutralino mixing matrix
  1  1  9.83389666e-01  # N_{1,1}
  1  2  -2.12816870e-02  # N_{1,2}
  1  3  1.68816482e-01  # N_{1,3}
  1  4  -6.31890094e-02  # N_{1,4}
  2  1  -1.54311193e-01  # N_{2,1}
  2  2  -5.20093774e-01  # N_{2,2}
  2  3  6.21972053e-01  # N_{2,3}

```

Figure 3.1: An example of supersymmetric particle parameters, in Les Houches format

3.2 Prospino

A particle's cross section is a factor in calculating the expected signal from a real-world collision [13]. Prospino performs the calculation of cross-sections, given the particles that are produced from proton+proton collisions, and the particles you are interested in measuring in the final state. It can produce accurate, next-to-leading order calculations, which is useful for calibration. However, for the thousands of parameter points required, Pythia includes a less accurate, leading order cross section in its simulation. It is more economical to use this in the general scans.

3.3 SoftSusy

The model of Supersymmetry used in this thesis is the Minimal Supersymmetric Standard Model (MSSM) - the least possible extension of the Standard Model that allows supersymmetrical particles. While it's the least extension, as mentioned above, it still has over 100 parameters. There are many models that constrain the parameters, but all these parameters still need to be used to solve for the physical particle masses. That is the purpose of a spectrum generator such as SoftSusy[14]. It generates the spectrum of particle masses and couplings from higher-level parameters. As in section 2.2.3 for example, the gaugino parameters are found in the gaugino “mixing matrices”. Calculating the gaugino masses then amounts to solving sets of matrix equations. SoftSusy does this quickly in many of the constrained models, as well as in the general MSSM.

3.4 Pythia

The two most computationally intensive and expensive tasks of the experiment are simulation of the collision and simulation of the detection. Pythia performs the first. A command file can be set up that gives general information about the event - the energy of collision, which particles are used to collide, which higher-order effects should be considered. This collider information and the SLHA file's model information are fed into Pythia. The first step in the simulation is generating all possible diagrams that might result from the collision [15]. It's worth noting for Chapter 4 and 5 that Pythia does not generate as many higher-order diagrams as a dedicated process generator. The second step is a Monte Carlo sampling of the dynamics of the system. One of the possible processes is selected randomly with a bias to the particles' decay rates. The four-vectors of the daughter particles are calculated, and the procedure begins again with this generation. The simulation terminates when all particles are "stable" (i.e. below some specified energy threshold that makes further decay simulation insignificant). This is repeated as required - often in the hundreds of thousands. After the repetition, Pythia will have produced a High Energy Physics Monte Carlo (HepMC) file that contains a snapshot of the vectors of all the final state particles.

3.5 Delphes

"The Pythia" was the title given to the head priestess, and the Oracle, of Delphi. So while Pythia produces the predictions, it is suitable that Delphes (the French for Delphi) simulates the place where the collisions occur - inside a detector. Delphes requires information about the particle states currently frozen in time in the detector, and the specifications of the detector to be simulated [16]. The former is parsed from a HepMC file. The latter is parsed from a Detector Card. This card contains information such as the detector's magnetic field, how precisely it can resolve levels and positions of energy, and how often it might mistake jets of particles for isolated particles.

Delphes takes the particle vectors and calculates how the particles would interact with the geometry of the detector. It is this "interaction" that registers as a particle being detected or not, depending on the sensitivity of the detector. Each of the signals is outputted in the same style as would come from a real detector, and this can be directly compared with real-world results.

3.6 Gambit

The Globular and Modular BSM Inference Tool (GAMBIT) is being developed at Adelaide University in order to provide a full package for performing analysis cuts on signals. It provides methods for quickly extracting particle data from the large and unwieldy Root files produced by Delphes. It runs on the intuitive object-orientated approach of C++ to treat each particle in the signal as a separate object. Thus, sorting into energy levels, calculating invariant masses, finding missing energy and so on is an accessible procedure.

The particular Gambit main program used in this thesis was almost entirely rewritten for the project. Information on the additions can be found in the next chapter.

3.7 Root

Root is a commonly used statistical package for particle physics [17]. It creates structures of n-tuples, and very naturally can produce n-dimensional histograms. It is made use of in three ways:

- The Delphes output is in Root format - this is unpacked by the Gambit software
- Likelihood calculations are done in tandem with Root, using its Poisson distribution methods
- The 10.8 million signals points are sorted into histograms within Root

4. Searching for Dark Matter at the LHC

We have seen so far the existence of Dark Matter, a hulking black spot in our understanding of the universe. We have also seen how the Minimal Supersymmetric Standard Model can account for this existence. In particular, the Lightest Supersymmetric Partner is the best candidate for Dark Matter due to its stability. The next section is then my original contribution to this theory: an experimental study of the parameters of candidate LSPs (candidates for the candidacy of Dark Matter, if you will). The candidates proposed are the neutralinos. And the properties to be explored are the four Susy parameters governing the gaugino masses M_1 , M_2 , μ and $\tan\beta$.

4.1 Event Measurement & Simulation

Overview

In the following two chapters, we are concerned with a process that should give a very clear indication of Beyond Standard Model physics: the 3 Lepton + Missing Energy signal. The two significant Susy production processes are seen in figure 4.1, both giving the same signal in slightly different ways.

The challenge in detecting the presence of a neutralino is differentiating the Susy process from background, SM processes and reconstructing the collision. A run of the experiment then consists of two main parts: simulating a pp collision, and looking for simulations that have tri-lepton signals. The second part is known as an “analysis cut”. We will discuss the analysis cuts first.

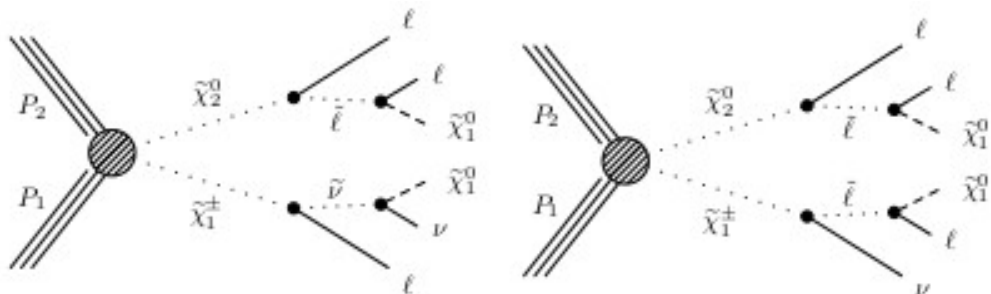


Figure 4.1: The two Susy processes we are concerned with

4.1.1 Detector Triggers

The layers of the CMS detector detect billions of particles each day. Many of these particles have negligible energy, and storing their information is a burden on a system already dealing with data in the tens of petabytes. There needs to be a procedure for discarding uninteresting and non-energetic collisions. This procedure is called *triggering*. In a physical detector, this is a combination of detector capability and event reconstruction. In a simulation, our detector can be arbitrarily sensitive, so we must specify lower energy limits on which events to register¹.

In the analysis, the following triggers are used:

- At least one electron or muon with transverse momentum $p_T^l > 17 \text{ GeV}$ and a second electron or muon with $p_T^l > 8 \text{ GeV}$
- Jets with $p_T > 10 \text{ GeV}$ are measured
- Pseudorapidity of leptons² $\eta < 2.4$
- Jets must have $\eta < 2.5$

4.1.2 Efficiency

The ability of a physical detector to measure a particle accurately and with precise resolution, like its energy trigger, depends on its construction. The rate of misidentification and jet detection describe the detector's *efficiency* E . It forms a relation with the detector's acceptance A :

$$A \times E = \frac{N_{\text{selected}}}{N_{\text{recorded}}}$$

The efficiencies enforced in the analysis were:

- A b-jet tagging efficiency of 70%
- Quarks lighter than b have a misidentification rate of 1%
- The resolution of lepton detection is $\Delta R = \sqrt{\Delta\eta^2 + \Delta\phi^2} = 0.3$.
- The resolution of jet detection is $\Delta R = 0.4$. That is, a lepton is considered isolated if separated by > 0.3 from other particles, and a jet isolated if separated by > 0.4 .

¹I denote "trigger" what is often called "primary trigger" - a quick check done at the level of detector hardware. What is often called a "secondary trigger" - the analysis-specific tests done at the level of reconstruction - is denoted "event selection" in this report

²In this chapter, "lepton" refers to an electron or muon - a tau decays hadronically and must be reconstructed separately

4.1.3 Event Selection

Once events have been triggered, and appropriate efficiencies and acceptances applied, the search can begin for Susy sensitive signals. First, events need to undergo a series of logical cuts specific to the tri-lepton final state. These cuts are:

1. There must be three leptons, or two leptons and a tau
2. At least one lepton has $p_T > 20$ GeV, and any others have $p_T > 10$ GeV
3. If a tau is present, has $p_T > 20$ GeV
4. The leptons must satisfy the extra isolation requirement that

$$I_{\text{rel}} = \frac{\sum p_T^{\text{Other Particles}}}{p_T^l} |_{\Delta R} < 0.15$$

5. Jets must have $p_T > 30$ GeV. These are not used as signal, but are used in testing the isolation of leptons
6. The event must have $E_T^{\text{miss}} > 50$ GeV¹
7. For channels 0-44, we require an Opposite-Sign, Same-Flavour pair of leptons. That is, and electron and positron, or muon and antimuon
8. The invariant mass M_{ll} is calculated using the OSSF lepton pair closest to the mass of the Z boson: 91.1876 GeV
9. The transverse mass is calculated using the third lepton's p_T

4.1.4 Background Events

The reason for choosing the most Z-like lepton pair to constitute the inverse mass is based on the likely backgrounds. The backgrounds discussed here are based on the simulation of [18], and summarised in figure 4.2. Considering only SM processes, the dominant diagram is 4.3. The interactions with the proton-proton collision result in a W^\pm producing a lepton $^\pm$ and a neutrino, which is recorded as missing energy. Therefore, this lepton is used in calculating transverse mass. As in Section 2.3.2, the transverse mass can be simplified in the case of an invisible partner.

A Z boson is also produced, which decays to a lepton-antilepton pair. This OSSF pair will have an invariant mass approximately equal to an onshell Z boson.

¹Events not satisfying this condition were still recorded as signal in a separate channel

Table 4.1: The set of OSSF observable bins

Flavour / Sign	M_{ll} (GeV)	M_T (GeV)	E_T^{miss} (GeV)	Channel
OSSF	< 75	0 – 120	0 – 50	0
			50 – 100	1
			100 – 150	2
			150 – 200	3
			200 – ∞	4
			0 – 50	5
			50 – 100	6
			100 – 150	7
			150 – 200	8
			200 – ∞	9
			0 – 50	10
			50 – 100	11
			100 – 150	12
			150 – 200	13
	> 75	> 160	200 – ∞	14
			0 – 50	15
			50 – 100	16
			100 – 150	17
			150 – 200	18
			200 – ∞	19
			0 – 50	20
			50 – 100	21
			100 – 150	22
			150 – 200	23
			200 – ∞	24
			0 – 50	25
			50 – 100	26
> 105	> 160	120 – 160	100 – 150	27
			150 – 200	28
			200 – ∞	29
			0 – 50	30
			50 – 100	31
			100 – 150	32
			150 – 200	33
			200 – ∞	34
			0 – 50	35
			50 – 100	36
			100 – 150	37
			150 – 200	38
			200 – ∞	39
			0 – 50	40
< 105	< 160	0 – 120	50 – 100	41
			100 – 150	42
			150 – 200	43
			200 – ∞	44

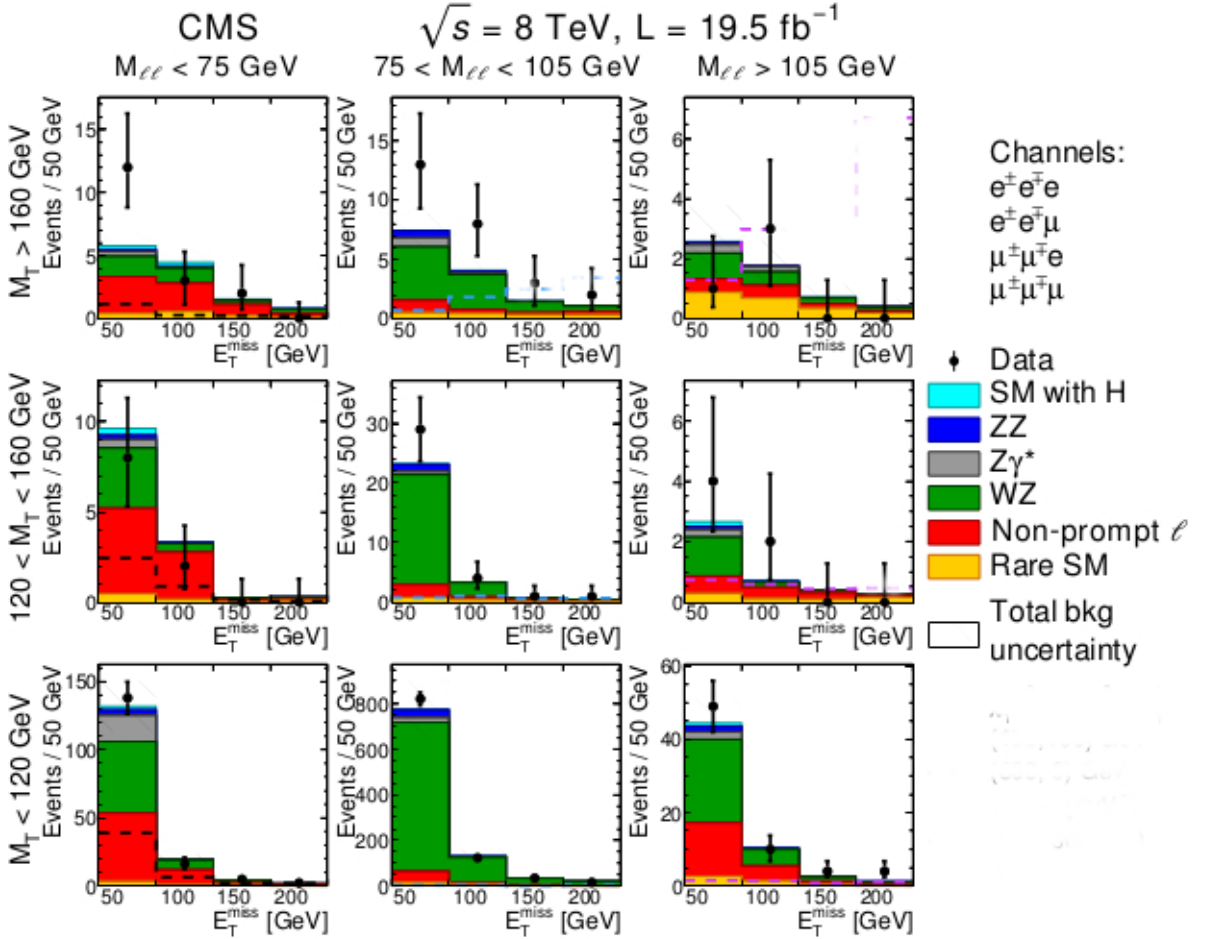


Figure 4.2: The significant Standard Model processes produce an OSSF trilepton event [18]

The reason the $3l + \text{MET}$ signal channel is so important is that the neutrino typically carries very little missing energy away from the process. Given an event with large MET, if we can accurately determine whether leptons have been produced via a Z boson or not, we can propose BSM physics as the production process. The viability of a particular set of process parameters then gives bounds on what neutralino masses might produce the observed signal.

4.2 Signal Analysis Calibration

CMS have produced a comprehensive scan of $\tilde{\chi}_1^0$ and $\tilde{\chi}_2^0/\tilde{\chi}_1^\pm$ masses at 8TeV [18]. They did this with tri-lepton signals, di-lepton signals, and W/Z signals, while making several simplifying assumptions. One was using a constrained version of Supersymmetry. Another was to set $m_{\chi_1^\pm} = m_{\chi_2^0}$, and parameterise $m_{\tilde{l}}$ as:

$$m_{\tilde{l}} = m_{\tilde{\chi}_1^0} + x_{\tilde{l}}(m_{\tilde{\chi}_1^\pm} - m_{\tilde{\chi}_1^0})$$

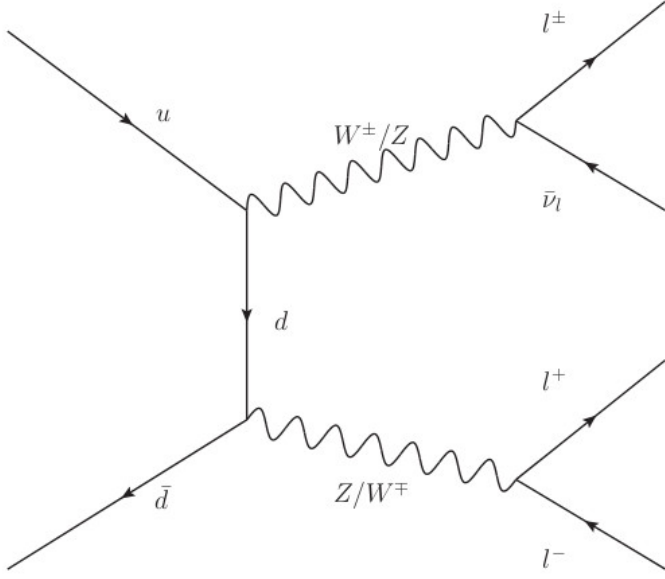


Figure 4.3: An example of how WZ production results in trilepton signals

For the calibration, $m_{\tilde{l}}$ was set to be the average ($x_{\tilde{l}} = 0.5$). These approximations serve to produce strong signals, as there is significant energy available for lepton production.

The signal cuts were organised in a way that made comparison with CMS LHC data straightforward (and this is the format I have continued to use for the more general scans).

I replicated these scans using an SLHA template scanning over $m_{\tilde{\chi}^{10}}$ and $m_{\tilde{\chi}^{20}} = m_{\tilde{\chi}^{1\pm}}$. Note that CMS did not release their SLHA files to me, despite gentle prompting. As such, several educated guesses needed to be made in order to closely reproduce their results. For example, (1) the gaugino mixing matrices used in the CMS study were unknown. Arbitrary matrices were used with the acknowledgement that production and decay rates may be sensitive to the mixing parameters. Initial comparison of the cross-sections using Prospino showed good agreement with CMS predictions - figure 4.4. Additionally, (2) a different simulation process was used, eschewing Madgraph in favour of the more economical Pythia for both diagram creation and dynamics. Find more detail on this in the next section. Finally, (3) analysis code was written to the specifications of the CMS paper.

This analysis code covers every possible signal channel. First, a given event was required to pass certain energy requirements, and to contain exactly three leptons and no more than one hadronic tau. Then, events were filtered into four channels based on flavour-sign topology, by testing for the presence and number of each lepton. Each of these channels was sorted into the bins of figure 4.1 for comparison with Standard Model data.

The following is a selection of the calibration scans compared to those produced by CMS.

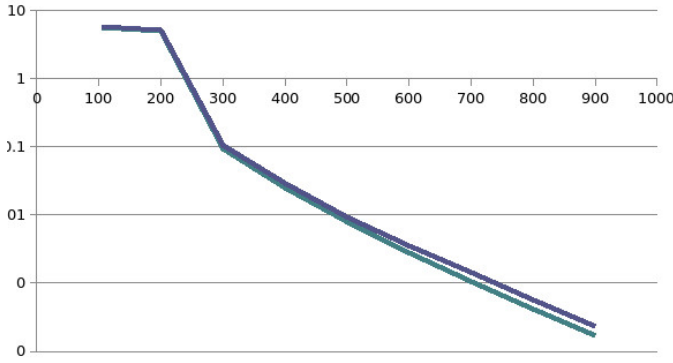


Figure 4.4: Comparison of simulated neutralino cross-section with CMS predictions

The first thing to note is these plots are representative the first is a good example of trilepton OSOF events, the second of tau-present events, and the third of OSSF events. It is clear that the latter two do not significantly duplicate CMS results. In fact, in some cases, they are as good as random. The possible sources of this disagreement are (1), (2) and (3) as mentioned above. In practice, the issue is likely a result of not comprehensively debugging this channel. The build of Pythia highly underproduces tri-lepton signals when taus have been produced. This is thrown as an “uncorrelated” error. The tau-absent channel, however, was exhaustively debugged and tested.

Given these sources of error, the tau-absent channels (figure 4.5a) can be said to be correctly calibrated. By introducing a systematic uncertainty that is likely a result of (1) and (2) these channels replicate CMS data to 20%, on average, for lower mass $\tilde{\chi}_1^0$ and $\tilde{\chi}_1^\pm/\tilde{\chi}_2^0$. Signals of tri-lepton states (i.e. electrons and muons) are then correctly simulated and correctly analysed by the analysis code. The signals can be used to produce branching ratios (by dividing by the total number of events, in this case 100,000). The number of events expected in the CMS detector is then given by:

$$N = \frac{N_{\text{simulated}}}{100,000} \sigma \mathcal{L}$$

These signal channels will be used to scan the general parameter space of gaugino masses, without making simplifying assumptions as in the CMS study.

4.3 Running The Experiment

Chapter two dealt with the physics of a supersymmetrical event, and this is used to determine the possible products of such an event and how they can be parameterised. Chapter three dealt with the computational tools to produce numerical predictions based on any collider physics. Now we are in a position to combine the computational tools with a specific set of

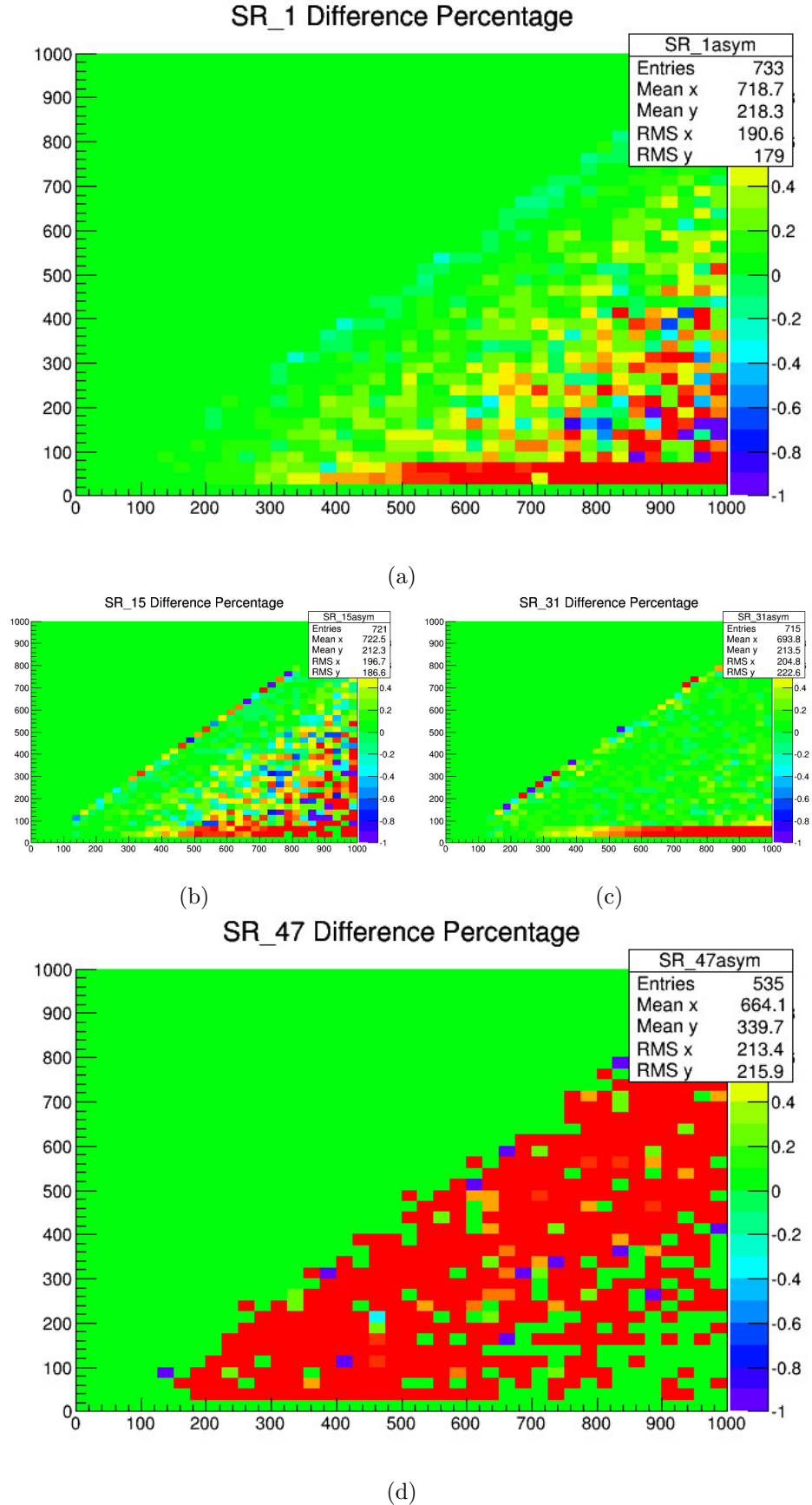


Figure 4.5: A selection of difference plots from the calibration process. One observes good agreement until channel 45 - the non-OSSF channels.

parameterised SUSY models. The following is a flowchart of how the experiment was run.

1. Parameter randomisation

Sample parameters randomly from a lognormal distribution¹. Ensures the values fully explore the lower energy values w/o neglection 1-2Tev parameters.
Scan over $0 \leq \tan \beta \leq 60, 0 \leq M_1, M_2, \mu \leq 2000\text{GeV}$

2. Assemble Parameter Files

The randomly generated parameters are inserted into N files in a format suitable for SoftSusy

3. SoftSusy

SoftSusy solves the gaugino mixing equations from parameter files, assuming a completely general MSSM model. All parameters, except for M1, M2, mu and $\tan \beta$ are decoupled in order to ignore non-electroweak SUSY interactions. N SLHA files are produced.

4. Cloud Job Script

A script makes N copies of Pythia, Delphes and the Gambit analysis. It then submits N jobs to the cloud, each running steps five to seven.

5. Pythia

Pythia is made to simulate 50,000 events from the random SLHA. All hadronisation is enabled. Additionally, a script reads in the Pythia log file and finds the relevant particles' cross-sections. Stores this with the parameters.

6. Delphes

Delphes is fed the HepMC file from Pythia and a detector card. The card has been altered to the specifications of the CMS detector. These include: Magnetic field=3.8Tesla, jet reconstruction using anti-kt algorithm with parameter R = 0.5, b-jet tagging efficiency of 70% and light-quark jet misidentification rate of 1%. A ROOT file containing all detected particle n-tuples is produced.²

¹Uniformly, in the case of $\tan \beta$

²This is not entirely how it ended up...

7. Gambit

The ROOT n-tuples are parsed into the runAnalysisOn-DelphesFile executable. This is made from a custom-written code for the scan. The custom code tests for the presence of precisely three leptons (with at most one tau). A series of logic tests find the leptons closest to Z mass, and calculates the invariant mass M_{ll} and transverse mass M_T based on the finding.

Finally, the code sorts the signal into charge/family structure (OSSF, OSOF, SS+tau, OSOF+tau), value of M_{ll} (0-75GeV, 75-105GeV, 105- ∞ GeV), value of M_T (0-120GeV, 120-160GeV, 160- ∞) and value of E_T^{miss} (0-50GeV, 50-100GeV, 100-150GeV, 150-200GeV, 200- ∞ GeV). (These bins are written to a text file. There are 180 ($4 \times 3 \times 3 \times 5$) signal channels, which reflect those in the CMS paper

8. Likelihood Testing

A numerical Gaussian integrator applies the systematic uncertainties to a Poisson likelihood test

9. Root

The signals and their respective likelihoods are concatenated into one text file and fed into ROOT. Here, we can produce 4-dimensional histograms, and isosurfaces of equal confidence limits. e.g. A surface around the parameters that give signals within two standard deviations of the observed signals.

4.4 Likelihood Testing

To be clear, the “experiment” detailed above is neither entirely experimental nor entirely theoretical. It is a numerical prediction of signal detection in a real-world experiment. That is, background signal can be generated (which is experimentally established with great confidence) and foreground SUSY signal can be predicted. These can then be compared with the corresponding signal channels in the CMS detector.

The comparison of prediction and measurement is called a “Likelihood Test”. Rather than simply comparing two numbers and their uncertainties, we have the extra information that the numbers were counted. This means that a signal of 30 actually contains 50,000 experiments, 30 of which were counted as “true” or “passed”. This style of test characterises a

Binomial or Poisson Distribution (depending on whether a theoretically-derived probability or an experimentally-derived mean signal value is used, respectively).

In order to test the significance of the generated signals, they are added to a generated background and compared to the observed signal. The predicted backgrounds and observations are listed in table 4.3. The channel can be cross-referenced to table 4.1.

Table 4.3: Background and observed CMS events

Channel	Background	Observed	Channel	Background	Observed	Channel	Background	Observed
1	132±19	138	16	776±125	821	31	45±7	49
2	20±4	16	17	131±30	123	32	10.0±1.9	10
3	4.0±0.8	5	18	34±8	34	33	2.5±0.5	4
4	1.9±0.4	2	19	21±7	14	34	1.2±0.3	4
6	9.6±1.7	8	21	23±5	29	36	2.7±0.5	4
7	3.3±0.8	2	22	3.4±0.7	4	37	0.71±0.22	2
8	0.26±0.10	0	23	0.72±0.19	1	38	0.38±0.14	0
9	0.29±0.11	0	24	0.36±0.12	1	39	0.24±0.20	0
11	5.8±1.1	12	26	7.5±1.4	13	41	2.6±1.2	
12	4.5±1.1	3	27	4.0±1.0	8	42	1.8±0.9	3
13	1.5±0.4	2	28	1.5±0.5	3	43	0.7±0.4	0
14	0.81±0.21	0	29	1.1±0.4	2	44	0.40±0.24	0

The likelihood of a signal is, in essence, the Poisson distribution at $x=\text{observed}$, with $p=(\text{signal}+\text{background})$ as the parameters, for a given channel. There are two complications, however. First, the parameters were not sampled uniformly. Second, there are systematic uncertainties to consider in the likelihood calculation.

4.4.1 Parameter Sampling

$\tan\beta$ was randomly sampled according to a uniform distribution, since there is no angle region of preference. On the other hand, μ, M_1, M_2 were sampled from a lognormal distribution:

$$P(x|s, m) = \frac{1}{\sqrt{2\pi}s^2x} e^{-\frac{(\log x - m)^2}{2s^2}}$$

Then, to span the full domain, this value $P(x)$ was taken to $10^{P(x)}$.

This was not due to a belief that the parameters *followed* this lognormal distribution. Rather that the values of immediate interest to LHC physics are in the ~ 1 TeV range, but that the higher ~ 2 TeV range shouldn't be ignored either. This distribution guarantees high sampling density for lower values, seen clearly in 4.6b.

While extremely useful to gather a wide range of parameters, we would like to convert back to uniform distribution after the likelihood for each parameter point has been calculated. This amounts to applying a series of reciprocal Jacobians to "unwrap" the transformations. This is then multiplied as a weighting to the histogram:

$$\frac{1}{\text{weight}} = \frac{1}{\mu} \cdot \frac{1}{\log \mu} \cdot e^{-\frac{(\log_{10} \log \mu - m)^2}{2s^2}}$$

An application of the transformation to figure 4.6b gives 4.6a. The higher masses contain lower sampling densities and therefore greater relative noise, but the likelihood can now be compared to a uniform distribution.

4.4.2 The Poisson Likelihood Function

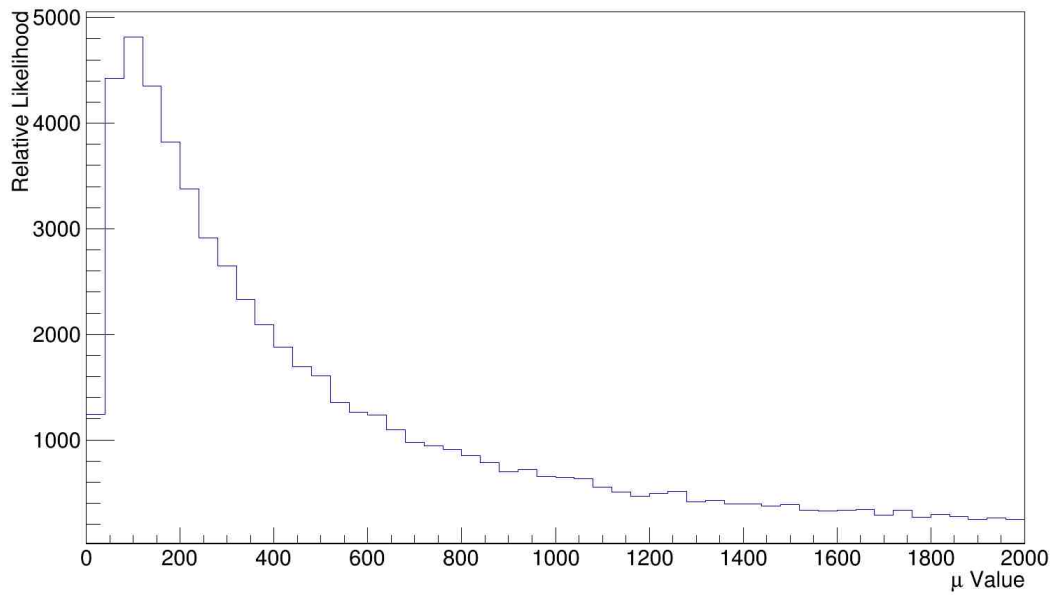
The Poisson probability distribution is given by

$$P(x|p) = \frac{p^x e^{-p}}{x!}$$

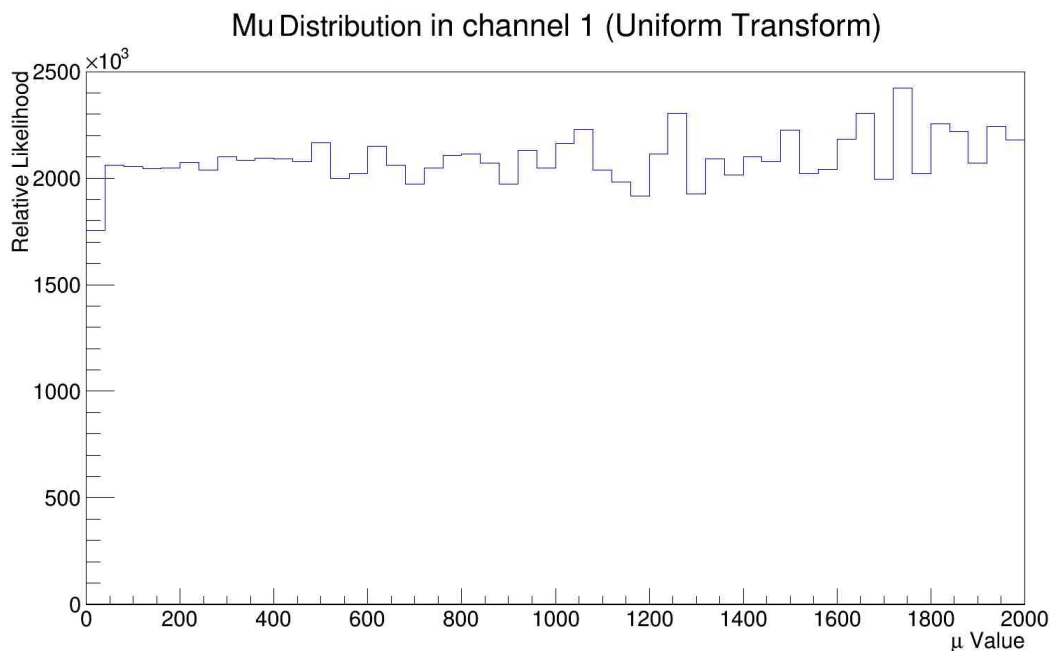
For the purposes of this project, the likelihood of a particular model being correct is less pertinent than the likelihood of it being *incorrect*. We are searching for exclusion limits, so are interested in likelihoods that are significantly low.

Additionally, there is a systematic uncertainty built into both background and signal numbers,

Mu Distribution in channel 1



(a) The randomly sampled 10^{\lognormal} distribution, i.e. likelihood = 1



(b) The transformed distribution returning the μ values to uniform distribution

Figure 4.6: An example of parameter transformation from distribution space to likelihood space

each 20% - 30%. We take the quadrature of these:

$$\Delta N_{\text{total}} = \sqrt{(\Delta N_{\text{background}})^2 + (\Delta N_{\text{signal}})^2}$$

and assume a normal distribution of these values around each point on the Poisson distribution. Thus, a likelihood calculation for each parameter point requires a numerical integration of one standard deviation over the composition of Gaussian and Poisson distributions.

4.4.3 Marginalisation

As this is a four-dimensional scan, it is impossible to look at a single point in 4D parameter space and say that it proves a particular parameter to be unphysical. Any or all of the parameters may be contributing to the likelihood. There are many complicated methods of "marginalising" or "profiling" all other parameters out, and getting a picture of how a 1D scan would look. In this project, we take a Bayesian approach and marginalise over the three remaining Susy parameters when viewing the 1D distribution for a particular parameter. This form of marginalisation is then implicitly integrating over the other parameters by histogramming.

5. Numerical Results

We now show the Bayesian posterior distribution for each of the four Susy parameters. In an attempt to highlight any exclusionary behaviour, the least likely of each bin was assembled into a **Least-Likely** histogram. That is, each histogram was looped over until the lowest, normalised set of bins was found.

To provide a visual correction to what may have simply been sampling bias, the **Least-Uniform** histogram is included. This is the histogram of lowest-count bins, with likelihood uniformly 1. That is, which of the bins in each of the 45 channels had the least sampling. This allows a comparison of random bias with true likelihood function behaviour. We are primarily interested in finding regions that can now be considered improbable and thus may be qualitatively excluded by the CMS searches. This will appear as a dip in the **Least-Likely** with respect to the **Least-Uniform**.

The μ distribution is given in figure 5.1. There is a noticeable divergence from the uniform distribution at low μ values. However, the dip is not large - the freedom of gauge couplings, which the other parameters determine, can still be chosen such that low mass models could evade detection. I also note that in the limit where $\mu \ll M_1, M_2$, a neutralino will become Higgsino-like.

The $\tan \beta$ distribution 5.2 is flat, as expected; consider that $\tan \beta = \frac{v_1}{v_2}$, where v_1, v_2 are the vacuum expectation values of the two Higgs doublets. The tri-lepton signature in the LHC is not sensitive to the Higgs sector, so we would expect it to follow a uniform likelihood.

In figures 5.3 and 5.4, the dip at low parameter values is more pronounced. The exclusion power in these scans is greater. As for μ , the lower parameters correspond to approximately bino and wino neutralinos, respectively. These may lead to more significant WZ+MET signatures.

Finally, in figure 5.5 we see the mass of the lightest neutralino. We see that there is no effective limit on the mass of the lightest neutralino from CMS searches. This is counter to a great body of literature.

The results do not break Susy. In general, they are as expected. With likelihoods that follow the sampling signal so closely, it is difficult to quantitatively produce an exclusion of parameters. Certainly, no parameters are excluded at the energies currently running at the LHC. The trade-off of sampling was simply that a lognormal bias gives a much faster, denser scan of the interesting parameter range. In return, there is a loss of statistically rigorous

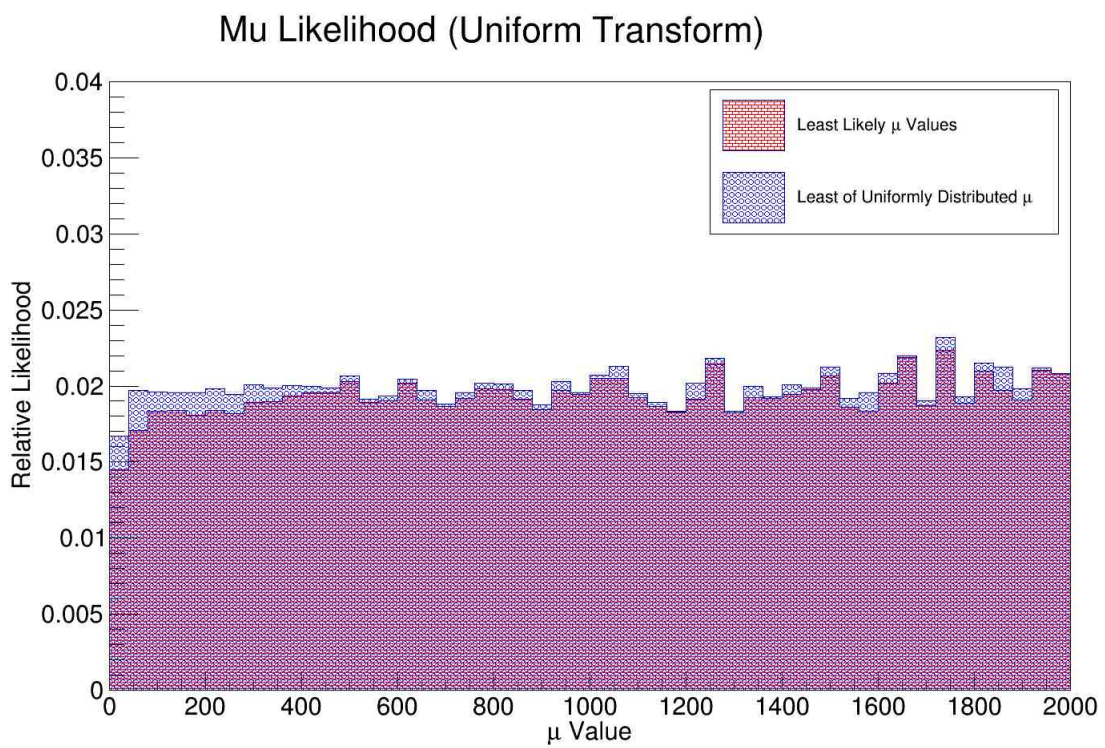


Figure 5.1

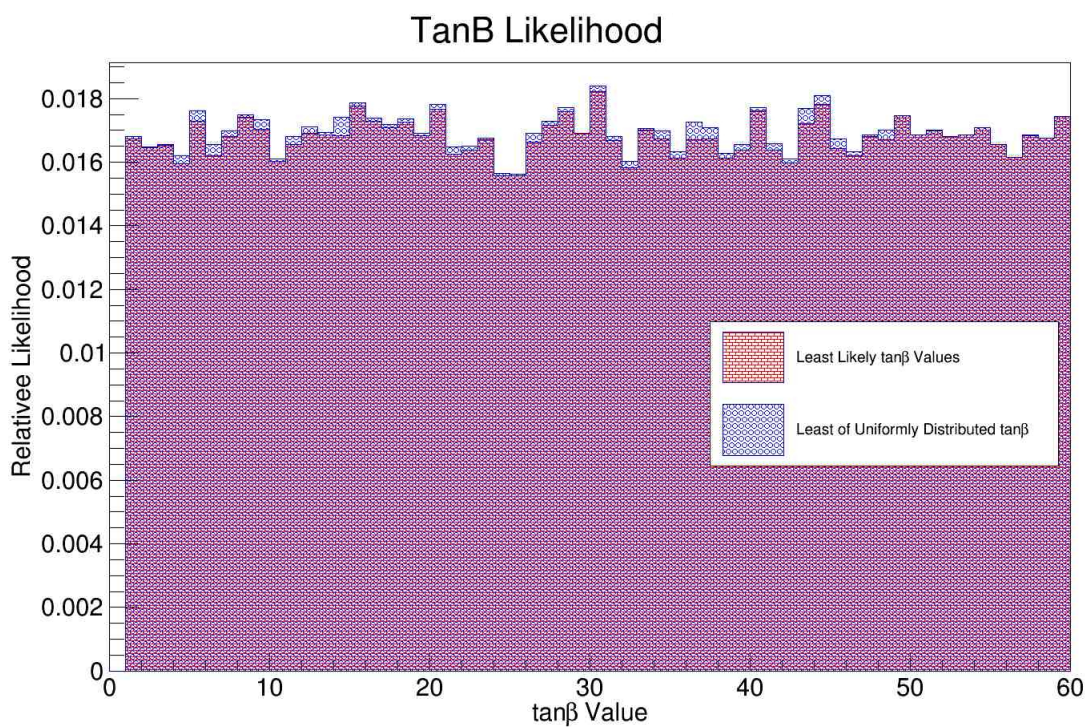


Figure 5.2

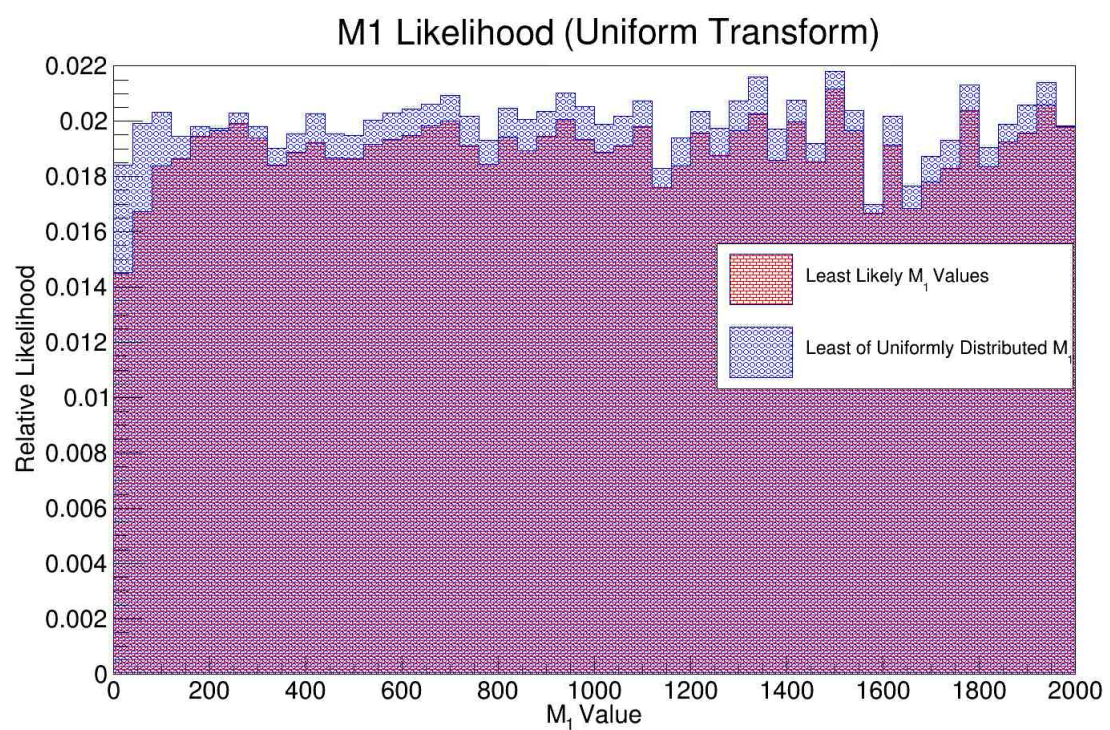


Figure 5.3

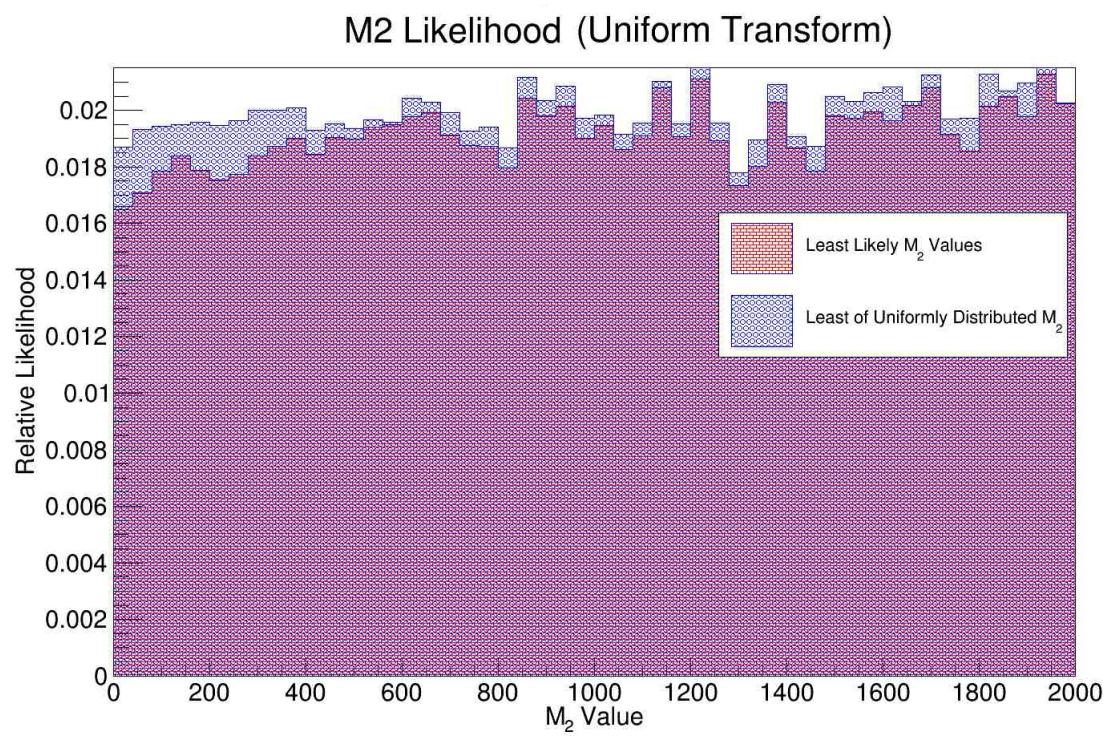


Figure 5.4

Mass Likelihood Distribution

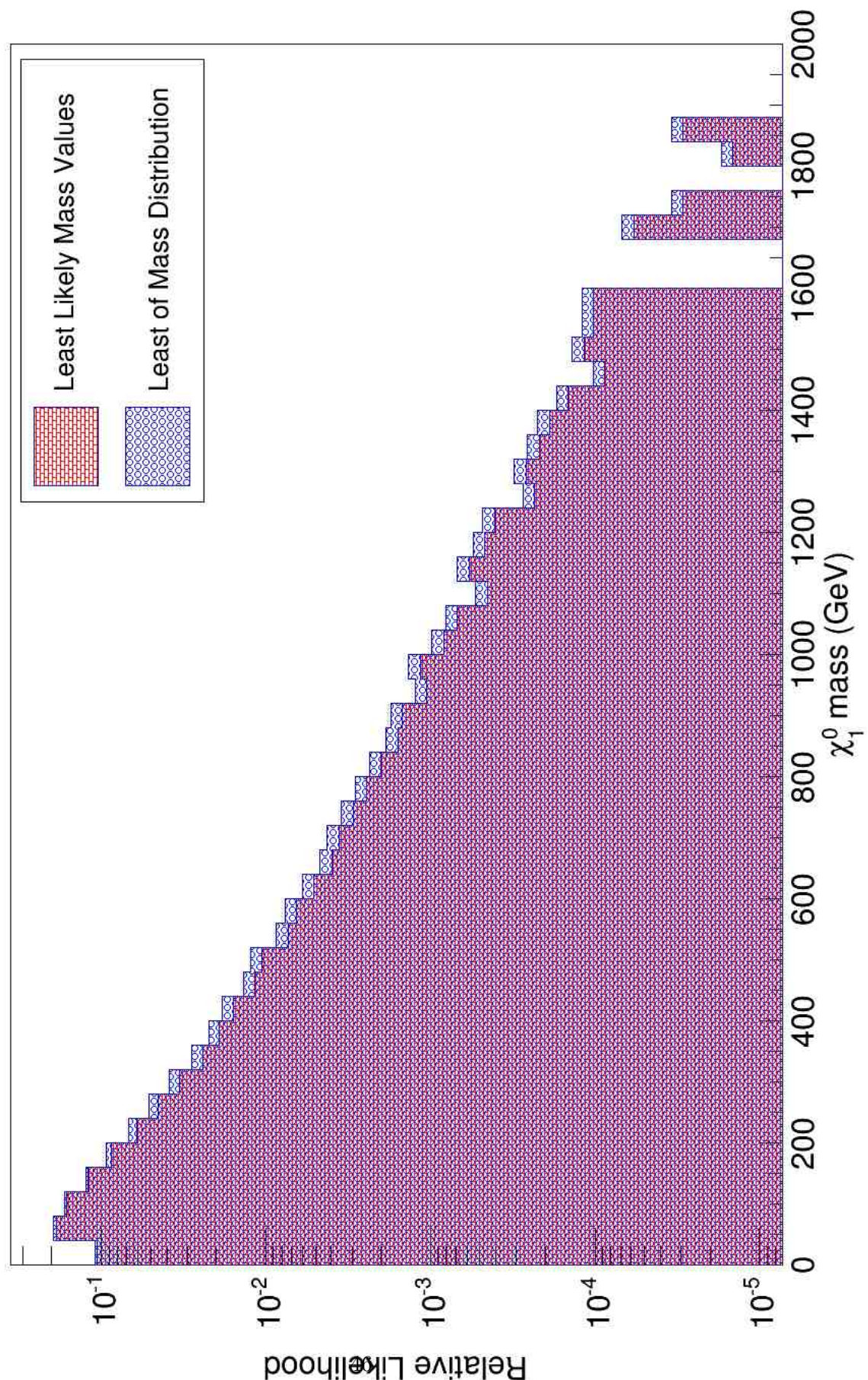


Figure 5.5

analysis. In particular, the sampling of the mass of the neutralino will follow a complex convolution of the four parameters' distributions, as seen in figure 5.5. It is not a trivial matter to transform this distribution to uniform.

6. Conclusion

Two outstanding physical problems from the 20th century, missing matter in the universe and the shortcomings of the Standard Model, have reached an unlikely convergence in Supersymmetry. By miraculous serendipity, Big Bang structure formation models propose a particle or particles that fit the profile of the supersymmetric gauge bosons. To uncover these particles, we simply extended the Standard Model with an extra symmetry - a symmetry of spacetime. This extension furnishes us with 25 super-particles, and a rich structure of unification. In spite of this elegance, Susy is coming under increasing criticism and pressure to deliver on its predictions. With the Higgs Boson predicted in 1964 and spectacularly discovered 48 years later, the popular science community may be in danger of expecting the same textbook discovery of other theories.

In spite of widespread prognostication of the death of Susy, this project has offered a measure of relief. Given the energies measured to date at the Large Hadron Collider, there is no reason to expect a clear observation of a neutralino. There is an indication that for lower energies the neutralino is becoming less likely. But there is no obvious exclusion of neutralinos even within the electroweak scale. Probing a theory such as Supersymmetry takes patience, and this report proposes that there is no basis for a negative prognosis of Susy. The results presented could certainly be extended to more rigorous analysis by taking a uniform sample of each of the four parameters. While time intensive, this method *may* allow exclusions to be placed on the parameter space.

An obvious extension is to properly calibrate all 180 signal regions. As mentioned in Section 4.2, tau-sensitive signals were miscalibrated, and so only a quarter of the available channels could be used with confidence. An exploration of the offending physics here will make an extra 135 channels of information available. These may contain exclusionary signals.

It may be that Large Hadron Collider collisions will not be sensitive enough to these candidate-LSP signals to produce narrow mass limits. If this is the case, we must look to astrophysics for (dis)proof of the Minimally Supersymmetric Standard Model, as they continue to gaze across the universe for Dark Matter.

References

- [1] G. de Vaucouleurs and K. C. Freeman, Structure and Dynamics of Barred Spiral Galaxies with an Asymmetric Mass Distribution, in *The Spiral Structure of our Galaxy*, edited by W. Becker and G. I. Kontopoulos, , IAU Symposium Vol. 38, p. 356, 1970.
- [2] E. Corbelli, mnras **342**, 199 (2003), astro-ph/0302318.
- [3] G. Bertone, D. Hooper, and J. Silk, Phys.Rept. **405**, 279 (2005), hep-ph/0404175.
- [4] G. Jungman, M. Kamionkowski, and K. Griest, Phys.Rept. **267**, 195 (1996), hep-ph/9506380.
- [5] S. D. McDermott, H.-B. Yu, and K. M. Zurek, Phys.Rev. **D83**, 063509 (2011), 1011.2907.
- [6] D. N. Spergel and P. J. Steinhardt, Phys. Rev. Lett. **84**, 3760 (2000).
- [7] B. Odom, D. Hanneke, B. D'Urso, and G. Gabrielse, Phys. Rev. Lett. **97**, 030801 (2006).
- [8] C. Beskidt, W. de Boer, and D. Kazakov, Physics Letters B , (2014).
- [9] M. E. Peskin and D. V. Schroeder, *An Introduction To Quantum Field Theory (Frontiers in Physics)* (Westview Press, 1995).
- [10] S. P. Martin, Adv.Ser.Direct.High Energy Phys. **21**, 1 (2010), hep-ph/9709356.
- [11] Particle Data Group, J. Beringer *et al.*, Phys. Rev. D **86**, 010001 (2012).
- [12] B. Allanach *et al.*, Comput.Phys.Commun. **180**, 8 (2009), 0801.0045.
- [13] W. Beenakker, R. Hopker, and M. Spira, (1996), hep-ph/9611232.
- [14] B. Allanach, Comput. Phys. Commun. **143**, 305 (2002), hep-ph/0104145.
- [15] T. Sjöstrand, S. Mrenna, and P. Z. Skands, JHEP **05**, 026 (2006), hep-ph/0603175.
- [16] DELPHES 3, J. de Favereau *et al.*, JHEP **1402**, 057 (2014), 1307.6346.
- [17] R. Brun and F. Rademakers, Nuclear Instruments and Methods in Physics Research Section A: Accelerators, Spectrometers, Detectors and Associated Equipment **389**, 81 (1997), New Computing Techniques in Physics Research V.
- [18] CMS Collaboration, V. Khachatryan *et al.*, Eur.Phys.J. **C74**, 3036 (2014), 1405.7570.